

**Quantifying vertical and horizontal stand structure using terrestrial LiDAR in  
Pacific Northwest forests**

Alexandra N Kazakova

A thesis submitted in partial fulfillment of the  
requirements for the degree of

Master of Science

University of Washington

2014

Committee:

L. Monika Moskal, PhD  
Miles Logsdon, PhD  
Dylan G. Fischer, PhD

Program Authorized to Offer Degree:  
School of Environmental and Forest Sciences

University of Washington

**Abstract**

**Quantifying vertical and horizontal stand structure using terrestrial and aerial LiDAR in Pacific Northwest forests**

Alexandra Kazakova

Chair of Supervisory Committee:  
Dr. L. Monika Moskal  
School of Environmental and Forest Science

Stand level spatial distribution is a fundamental part of forest structure that influences many ecological processes and ecosystem functions. Vertical and horizontal spatial structure provides key information for forest management. Although horizontal stand complexity can be measured through stem mapping and spatial analysis, vertical complexity within the stand remains a mostly visual and highly subjective process. Tools and techniques in remote sensing, specifically LiDAR, provide three dimensional datasets that can help get at three dimensional forest stand structure. Although aerial LiDAR (ALS) is the most widespread form of remote sensing for measuring forest structure, it has a high omission rate in dense and structurally complex forests. In this study we used terrestrial LiDAR (TLS) to obtain high resolution three dimensional point clouds of plots from stands that vary by density and composition in a second-growth Pacific Northwest forest ecosystem. We used point cloud slicing techniques and object-based image analysis (OBIA) to produce canopy profiles at multiple points of vertical gradient. At each height point we produced

segments that represented canopies or parts of canopies for each tree within the dataset.

The resulting canopy segments were further analyzed using landscape metrics to quantify vertical canopy complexity within a stand.

Based on the developed method, we have successfully created a tool that utilizes three dimensional spatial information to accurately quantify the vertical structure of forest stands. Results show significant differences in the number and the total area of the canopy segments and gap fraction between each vertical slice within and between individual forest measurement plots. We found a significant relationship between the stand density and composition and the vertical canopy complexity. The methods described in this research make it possible to create horizontal stand profiles at any point along the vertical gradient of forest stands with high frequency, therefore providing ecologists with measures of horizontal and vertical stand structure.

**Key Words:** Terrestrial laser scanning, canopy structure, landscape metrics, aerial laser scanning, lidar, calibration, Pacific Northwest

## Table of Contents

<b>List of Figures</b> .....	iii
<b>List of Tables</b> .....	v
<b>Acknowledgements</b> .....	vi
1. Introduction .....	1
1.1 Background .....	2
1.1.1 Forest Structure .....	2
1.1.3 Calibration of ALS with TLS.....	7
1.2 Research Goals and Objectives .....	8
2. Methods .....	9
2.1 Study Area.....	10
2.2 Terrestrial Laser Scanning .....	12
2.3 Aerial Laser Scanning .....	13
2.4 Field Data Collection .....	15
2.5 Derivation of Variables.....	15
2.5.1 Terrestrial Lidar Point Cloud Processing.....	15
2.5.2 Plot Point Cloud Slicing and Canopy Surface Creation .....	16
2.5.3 Canopy Segmentation and Classification .....	18
2.5.4 Extraction of Canopy Metrics.....	21
2.6 Field Plot Metrics .....	24
2.6.1 Density .....	24
2.6.2 Composition.....	25
2.6.3 Aboveground Tree Biomass and Canopy Mass .....	25
2.6.4 Processing Aerial LiDAR.....	29
2.7 Analysis .....	29
2.7.1 Stand Structure from TLS .....	29
3. Results .....	35
4. Discussion .....	45
4.1 Sources of Error .....	49

5. Conclusions .....	50
5.1 Future Research .....	51
Bibliography .....	52
Appendix A: List of acronyms .....	57
ASCII: American Standard Code for Information Interchange .....	57
BLM: Bureau of Land Management.....	57
GIS: Geographic Information Systems.....	57
Appendix B: List of definitions .....	58
<i>TLS</i> – Terrestrial laser scanning .....	58
<i>Richness</i> – the number of different patch types .....	58
Appendix C: Metadata.....	60

## List of Figures

<b>Figure 1.</b> A graphic representation of the Pacific Northwest forest in a vertical diversification stage. The blue line represents the canopy structure that can be obtained with ALS and the red line represents the canopy structure complexity that is omitted by ALS and can be captured and quantified by TLS. Illustration by Robert Van Pelt .....	4
<b>Figure 2.</b> Flow chart for canopy vertical and horizontal structure quantification and comparison of TLS versus ALS approach.....	10
<b>Figure 1.</b> A. Map of Oregon State and location of the Panther Creek Watershed. B. Locations of TLS plots within the PCW study area, where the yellow dots represent plots that have been scanned from 4 locations and blue dots represent plots that have been scanned from the center location only. The blue dots represent plots with slopes over 30 degrees. Due to topography these plots were scanned from center locations only. The map of Oregon was created by <a href="http://www.maps.com">www.maps.com</a> .....	11
<b>Figure 4.</b> TLS scanner set up schematic for scanning in forested environments of dense Pacific Northwest forests. The purpose of multiple scan locations within the plot is to minimize the laser shadow effect and obtain a good 3D representation of the entire plot. (Moskal 2011, unpub.) .....	13
<b>Figure 5.</b> Three dimensional point cloud of Panther Creek Watershed colored by RGB values from NAIP imagery. (Watershed Sciences Inc., 2010) .....	15
<b>Figure 6.</b> Digital terrain model of one of the study plots.....	16
<b>Figure 7.</b> TLS point cloud slicing schematic .....	17
<b>Figure 2.</b> Plot TLS point cloud canopy slice: from top left to bottom right are the heights represent the lowest and the highest points of each slice for that particular plot.....	19
<b>Figure 9A.</b> Object based image analysis step by step graphic.....	20
<b>Figure 3B.</b> Visual representation of the TLS point cloud processing.....	21
<b>Figure 4.</b> Canopy distribution maps (canopy polygons segmented and classified in eCognition) for one of the study plots.....	23
<b>Figure 11 A.</b> Differences in point cloud densities between the TLS and ALS. Raw point counts for 5 sample plots from TLS scans ( <b>B.</b> ) and ALS scans ( <b>C.</b> ).....	33
<b>Figure 12.</b> Canopy points (%) distribution along the height gradient (along the canopy slices (1-6)) for 5 example plots.....	34
<b>Figure 13.</b> Average canopy point distribution for TLS and ALS.....	35
<b>Figure 14.</b> Scree plot of principal component analysis (PCA).....	36
<b>Figure 15.</b> PCA Ordination.....	37
<b>Figure 16.</b> Multivariate Regression Tree.....	39
<b>Figure 17.</b> NMDS ordination of plot canopy structure metrics by canopy slice.....	41
<b>Figure 18.A</b> NMDS ordination of canopy structure metrics.....	42
<b>Figure 19.</b> NMDS ordination of canopy structure metrics for ALS and TLS derived canopy patches.....	44
<b>Figure 20.</b> The graphic shows mid-canopy slices of three distinctive plots in respect to the tree density.....	47

**Figure 21.** Raw point clouds for mid-canopy slices for two plots with similar densities but different compositions.....48

## List of Tables

<b>Table 1.</b> Aerial LiDAR survey specifications .....	14
<b>Table 2.</b> List of patch metrics used to describe canopy structure derived from TLS point clouds.....	24
<b>Table 3.</b> sdi classification scheme.....	25
<b>Table 4.</b> List of Biopak formulas used to calculate aboveground tree biomass.....	26
<b>Table 5.</b> List of Biopak formulas used to calculate canopy biomass.....	26
<b>Table 6.</b> Summary of explanatory variables used for analyses.....	27
<b>Table 7.</b> Environmental variables derived from the field measurements summarized by plot.....	28
<b>Table 8.</b> First three Principal Components (PC1, PC2, and PC3), and the loadings of each component.....	38
<b>Table 9.</b> PerMANOVA results.....	42
<b>Table 10.</b> PerMANOVA and ANOVA results, significance levels.....	43



## **Acknowledgements**

This research has been supported by Bureau of Land Management (BLM) Washington/Oregon, and carried out in the UW Remote Sensing and Geospatial Analysis Laboratory (RSGAL).

Thank you to my committee, L. Monika Moskal, PhD (chair), Miles Logsdon, PhD, and Dylan G. Fischer, PhD, for providing me with assistance and advice based on their expertise.

Thank you to the Bureau of Land Management (BLM) of Oregon and Panther Creek Watershed Science Consortium for providing data: list the agencies and what they provided. The Precision Forestry Cooperative at UW is acknowledged for providing research resources such as field equipment and administrative assistance.

A special thank you to Justin Kirsch and Riley Milinovich for spending the summer collecting Terrestrial LiDAR data in the Panther Creek Watershed.

Many thanks to Meghan Halabisky, Jeff Richardson, Michael Hannam, that helped me out and other members of RSGAL for advice, humor and camaraderie.

Most importantly I would like to thank my family, my partner Brandy Ranger, my son Kirill Huizenga and my mother Larisa Kazakova, who have supported me through this endeavor and have helped make this work possible.

## 1. Introduction

Stand structure is defined as the spatial arrangement of the components of vegetation (Lincoln et al. 2003). Forest stands can be described by horizontal and vertical structure. Horizontal structure represents a spatial distribution of individual trees and vertical structure describes the spatial vertical distribution of canopy. The vertical structure of tree communities is formed by the variations in growth forms or tree physiognomy (Kimmins 1997). There are many variables that cause variability in stand vertical and horizontal structure, most important being stand age, succession stage, and composition.

Stand structure is not static; it is a constantly changing part of forest ecosystem. Forests are continuously subject to disturbances at many scales, ranging from death of an individual tree within a stand to high severity fires that wipe out large forest communities. The diversity of type and frequencies of natural disturbances lead to a high diversity of structural conditions: from even-aged, single species stands to multi-age, compositionally diverse, multilevel canopy forest structures. Stand structure reflects ecosystem's resistance and resiliency to disturbance. An ecosystem's recovery from a disturbance is one of the factors that determine the structural arrangement of trees as the stand progresses through the stages of development from stem initiation to stem exclusion, to vertical and horizontal diversification (Van Pelt 2007).

The spatial pattern of tree distribution within a stand is particularly important as it is a key factor in predicting and modeling a stand's potential resistance to a disturbance. It has been shown that stands that are less dense with randomly distributed trees are less susceptible to the spread of insect damage. Trees that are clumped together and whose canopies intersect are much more likely to facilitate the spread of spruce budworm and mountain pine beetle (Campbell et al. 2007). Diverse vertical structure creates fuel ladders that are important in predicting fire dynamics potential on the landscape (Cruz et al. 2003). Assessing stand horizontal and vertical structure can help predict the stands susceptibility to various types of disturbances.

The change in stand structure is highly important in creating habitat for a variety of animals. Each particular structure offers unique habitat features. Forest canopy vertical structure and distribution can provide key information for avian habitat modeling. Many habitat suitability models depend on canopy structure and stand density. For example a habitat suitability model that was built for black capped chickadees includes a combination of tree heights and canopy closure (Schroeder, 1983). Certain species of birds prefer to nest in canopies of various structures and densities, for example endangered marbled murrelets solely depend on older canopies with complex and very particular branch structure for finding suitable nesting platforms. Red tree voles and other small canopy dwelling mammals depend on canopy structure with high connectivity as it allows for their movement from tree to tree within their range. Maintaining structural diversity within forest ecosystems is extremely important for maintenance and promotion of high landscape-level wildlife diversity. Canopy structure can also be linked to stand productivity both above and below ground (Kirsch 2013). Canopy distribution along a height gradient can provide us with canopy porosity, light attenuation, and correlated with understory biomass. The ability to quantify canopy structure gives researchers and land managers valuable knowledge about habitat suitability and arms the policymakers with very important information in attempts to strike a balance in protecting the endangered species and their habitat while managing the forest resources.

## **1.1 Background**

### **1.1.1 Forest Structure**

The importance of structural complexity in forest ecosystems and diversity have been acknowledged, where the increasing structural complexity in forests enhance their ecological complexity and therefore the foundation for maintaining high biodiversity (Rapp, 2003, Michel and Winter, 2009). We can use vertical structure complexity to describe stand level canopy dimensions which are useful in many forest management decisions including wildlife habitat value and monitoring forest health. There are many ways that

canopy dimensions can be measured in the field. Crown dimensions are also used to estimate multiple parameters including crown competition factor, crown density, crown surface area, live crown ratio, volume. Measuring crown parameters in the field can be a challenging and time consuming task, often prone to high measurement error. Crown diameters can be measured for individual trees within the plot by projecting the perimeter of the crown vertically to the ground and taking measurements of these projections. This method is extremely time intensive and is difficult in higher density forests with multi-layered canopies, due to visibility restrictions. Various instruments that measure the projection of crowns in the plot exist (e.g. right-angle prism densitometer or a spherical crown densitometer), where devices measure a reflection of the canopy directly above and where a slight change in viewing angle can significantly over or underestimate the canopy cover estimates (Fiala et al. 2006).

Crown diameters can also be measured using remote sensing techniques. There are some commercially available instruments that can be used for obtaining canopy structural information indirectly. These sensors can be categorized into linear and hemispherical. One of the oldest and widely used is the use of vertical aerial photographs, or hemispherical photographs, where the crown cross-sectional area is calculated from the formula for the area of a circle using either the average of the maximum and the minimum crown diameters, two diameters at right angles, or from the maximum diameter and another at right angles to it (Richardson et al. 2009).

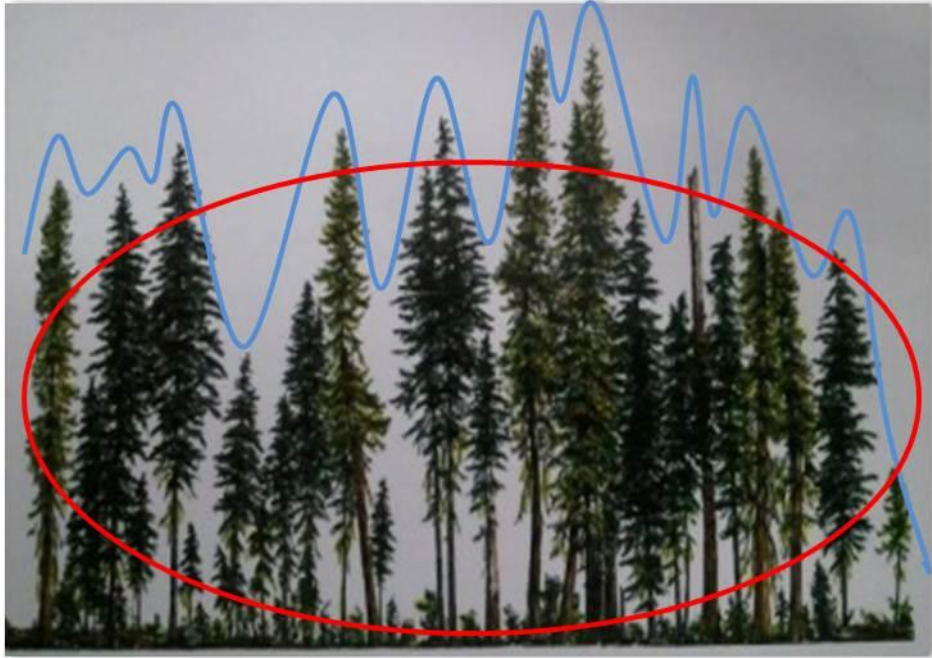


**Figure 5.** A graphic representation of the Pacific Northwest forest in a vertical diversification stage. The blue line represents the canopy structure that can be obtained with ALS and the red line represents the canopy structure complexity that is omitted by ALS and can be captured and quantified by TLS. Illustration by Robert Van Pelt

### 1.1.2 Remote Sensing

Remote sensing is the science and art of obtaining information about an object, area, or phenomenon through the analysis of data acquired by a device that is not in contact with the object, area, or phenomenon under investigation (Lillesand et al. 2008). Remote sensing links spatial patterns and ecological processes at multiple scales: spectral, spatial and temporal. Remote sensing has facilitated great advances in the mapping, modeling and understanding of ecosystems. There are two types of remote sensing: passive and active. Typical and most widely used type of remote sensing in ecosystem studies is passive optical remote sensing from aerial photography and satellite imagery (Goward and Williams 1997). Photogrammetric remote sensing techniques

have been very successful at classifying and mapping the ecosystem components such as landforms, water bodies and vegetation. Aerial imagery has been used to map forest stands and fragmentation of forests. Active remote sensing involves the use of active sensors, such as radar or lidar, which transmit their own energy and then record the signal reflected back to the sensor from the target.

### **1.1.2.1 LIDAR**

#### **1.1.2.1.a Aerial Light Detection and Ranging (LiDAR)**

Technological advancements in the field of remote sensing including the development and implementation of hyperspatial Light Detection and Ranging (LiDAR) and hyperspectral remote sensing are driving the discipline to new frontiers of forestry applications. LiDAR is one of the active optical remote sensing technologies and is a great tool for extracting information about vertical and horizontal canopy structure by measuring distance by time-of-flight using pulsed laser light (Bufton 1989). According to Lefsky et al 2002, there are two main types of LIDAR systems used in remote sensing of vegetation, waveform-recording and discrete return. Waveform-recording systems measure the vertical distribution of the intercepted canopy surfaces and the underlying ground surface within a single footprint using high-speed digitization of the backscattered return from a short duration laser pulse (Harding et al. 2001). Discrete-return LIDAR systems measure the distances to one or a few surfaces in a small diameter spot from which the backscattered laser energy exceeds a detection threshold (Parker et al.2004). The three dimensional nature of LiDAR data makes it possible to detect and isolate individual and clusters of trees (Hyypä et al., 2001; Persson et al., 2002; Samberg and Hyypä, 1999). Sumnal et al. 2012, have successfully used both small-footprint discrete return and full waveform aerial LiDAR to estimate forest inventory parameters. Discrete-return LIDAR has been widely used in terrain mapping (Baltsavious 1999), but it has also been used for research of vegetation canopies (Rithchie et al. 1993; Parker and Russ 2004).

### 1.1.2.1.b Terrestrial LiDAR

Although the ALS has been widely used in estimating the ecosystem parameters, the use of TLS in forest ecology and ecosystems studies is a rather new and under-developed area. Although ALS is great at capturing coarse estimates of stand vertical structure over large areas it falls short at capturing the complexities of structure that are associated with multi-layered canopy of vertically and horizontally structurally complex stands of Pacific Northwest. Terrestrial LiDAR is great at capturing stand structure from ground up and compensates ALS at certain level.

Due to its highly detailed three dimensional quality, TLS data holds great potential for highly accurate estimates of forest's vertical and horizontal structural components both on the individual tree and stand levels. The use of TLS in forest practices is a relatively new development. The potential of terrestrial lidar scanners for plot vegetation characterization has been tested by a number of researchers with varying degrees of success. Most of the previous studies of vegetation using TLS have been focusing on extracting individual tree parameters such as diameter at breast height (DBH), height, height to live crown, crown diameter etc. (Hopkinson et al., 2004; Moskal and Zhen, 2001; Pueschel, 2013). Many attempts were made to reconstruct individual trees by creating three dimensional models from the high density point clouds. Watt and Donoghue 2005 were able to successfully measure DBH, upper stem diameters and branch intermodal distance in dense Sitka spruce plantations using TLS. Jupp et al. 2009 were able to measure leaf area index (LAI) using a cutting edge EchinDNA scanner, which is a full waveform recording, multi-view, angle scanning lidar system. The same instrument was used to retrieve forest stand structural parameters, including mean DBH, stem count density, basal area, and above-ground woody biomass with very good accuracy in New England conifer and hardwood forest stands (Yao et al., 2011). Liang et al. 2012 successfully (73% accuracy) attempted to automate the stem mapping using TLS in relatively dense mixed forest of Finland. Antonorakis et al. 2009 were able to use TLS



point cloud to determine the roughness of vegetation with different structure characteristics for use in resistance equations and flood modeling, by creating voxel based representations of leafless tree structures in poplars.

The common theme for the previous studies in attempt to characterize forest structure from TLS is the use of individual tree parameters approach. Although this approach works well in many stands it is very difficult to apply in dense and multi-layered stands of Pacific Northwest. The complex vertical and horizontal structure of conifer and mixed stands cause difficulties in separating individual tree canopies even with multiple vantage points high resolution stitched scans, therefore increasing the uncertainty within canopy structure parameters. A different approach that focuses on quantifying canopy structure on the plot or even stand level is needed. Here I use the combination of both TLS and ALS to quantify the structure and distribution of multi-layered complex canopy of the dense stands of Pacific Northwest.

### **1.1.3 Calibration of ALS with TLS**

There are several limitations to the utility of aerial LIDAR alone for the investigation of canopy structure. The relatively large diameter laser beam size (0.5-1m) means that for closed canopies it will be intercepted by the canopy surface and will not penetrate through the top layer to adequately describe canopy structure beyond the surface. It is very common to simply discard second and third returns from the discrete-return dataset to simply build a canopy surface model out of first returns and to estimate canopy structure (See Figure 1.). Terrestrial LIDAR provides the structural information that is missed by the aerial systems, where it captures canopy structure from beneath the canopy, but has a difficult time penetrating through the entire canopy for accurate canopy surface estimates. Although TLS systems are good at quantifying canopy structure along a vertical gradient it is often limited to small areas. Terrestrial LIDAR units are often bulky and cannot be carried for long distances. The scanner systems are also stationary and require some time for

each acquisition. The active scanning time depends on the type of the scanner and the desired resolution and quality of the point clouds. The data acquisition time is dependent on the number of scans needed for the accurate representation of the plot, minimizing error due to obstruction by vegetation. Hopkinson et al. 2013 have successfully established a relationship between the TLS derived (Echidna Validation Instrument) LAI profile and ALS foliage percentile distribution in mature eucalyptus forests of New South Wales, Australia. The TLS approach works well for acquiring canopy structure information on a small scale and is not practical for large area acquisitions. However highly detailed three-dimensional canopy structure information derived from small areas with TLS systems can be used to calibrate the structural information collected with aerial systems. The resulting model can be then further used to quantify and interpolate canopy structure over large areas and provide necessary information to answer a number of landscape level ecological questions.

## **1.2 Research Goals and Objectives**

The main goal of this study is to use remote sensing techniques to quantify stand level canopy structure. Specifically to develop a method that uses TLS point cloud to accurately quantify canopy vertical and horizontal distribution within each of the study plots. The idea is to utilize TLS derived datasets in such a manner that makes it unique to TLS, to take advantage of the full potential of the tree dimensional spatially explicit datasets provided by the scanner. The goal is to come up with a relatively simple method of accurately quantifying a stand's canopy structure that can be easily applied for a wide array of ecosystem studies. To achieve this goal I identified the following objectives:

- 1) Develop a method of processing a TLS point cloud of a plot that helps us estimate canopy spatial distribution along a vertical gradient of the stand.

- 2) Describe and quantify the canopy distribution along a vertical gradient using landscape/patch metrics.
- 3) Explore the variability of canopy structure complexity within and between stands.
- 4) Explore the change in canopy structure complexity with changes in stand's composition, density and aboveground biomass.

Second goal of this research is to explore the possibility of using canopy structure metrics obtained with TLS to model the structure components obtained using ALS

- 1) Apply an above mentioned method to ALS point cloud data
- 2) Explore the vertical gradient results for both and determine the optimal height at which both TLS and ALS describe the canopy structure
- 3) Develop a model that can be used to calibrate canopy structure derived from ALS using canopy structure metrics derived from TLS point cloud data.

## **2. Methods**

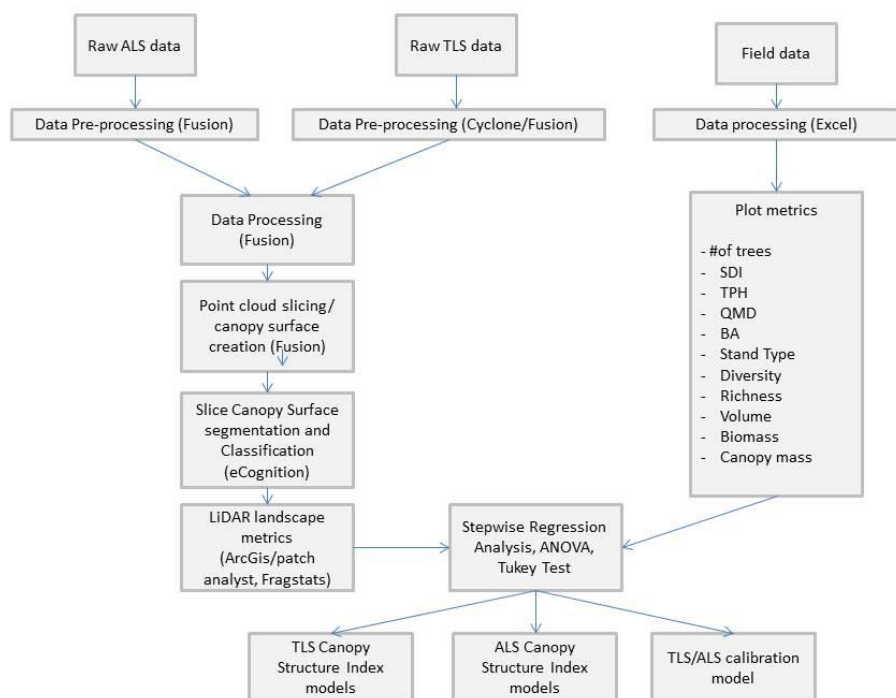


**Figure 6.** Flow chart for canopy vertical and horizontal structure quantification and comparison of TLS versus ALS approach.

## 2.1 Study Area

Panther Creek watershed is a 2300 hectare forested watershed in the coastal mountain range of Oregon, USA. Panther Creek watershed ( $45^{\circ}18' N$ ,  $123^{\circ}21' W$ ) is at an elevation of 100-700 m. Panther Creek Watershed (PCW), is located in the Yamhill County, Oregon, approximately 80 km west of Salem, OR and about 57 km southeast of Portland. Annual precipitation is about 150 cm. The forests are mainly planted or natural stands of Douglas fir, with significant amounts of western hemlock, western red cedar, grand fir, red alder, big leaf maple and several other species. Tree heights are up to 60 meters. Management intensity throughout the watershed has been variable, with varying planting densities, and both thinned and unthinned regimes. The ecoregion is classified as “Cascade mixed forest”. It is in the eastern part of the coastal range

physiographic province of Oregon state. The forests of northwestern Oregon belong to mesic temperate coniferous type. The environment is mild and extremely favorable for forest development. The study area is dominated by native species: *Pseudotsuga menziesii* (Mirb.) Franco, *Tsuga heterophylla* (Raf.) Sarg., *Thuja plicata* Donn ex D. Don, *Acer macrophyllum* Purs., and *Alnus rubra*.

Panther Creek Watershed is part of US Bureau of Land Management (BLM) intensive Panther Creek experimental research program. The collaborative research projects involve over thirty agencies and companies with interests in broader questions of forest management and ecosystem management (Flewelling, 2012). (Fig. 3.A) The study area spans 5,580 acres and represents a natural, previously managed, heterogeneous forest ecosystem.

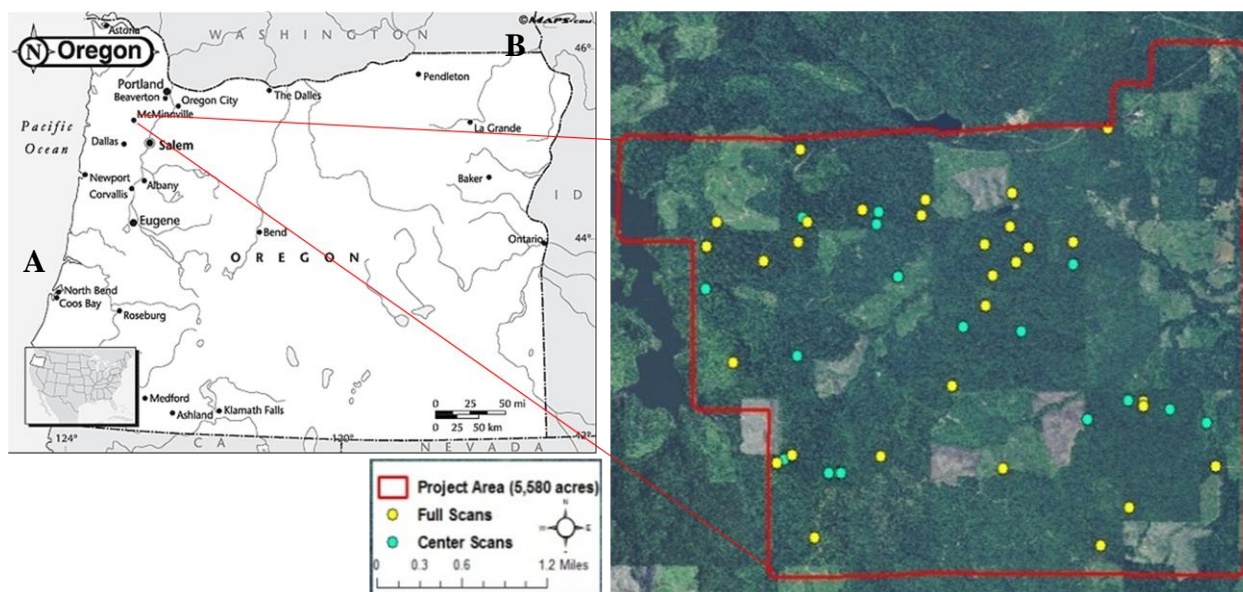


**Figure 7.** A. Map of Oregon State and location of the Panther Creek Watershed. B. Locations of TLS plots within the PCW study area, where the yellow dots represent plots that have been scanned from 4 locations and blue dots represent plots that have been scanned from the center location only. The blue dots represent plots with slopes over 30 degrees. Due to topography these plots were scanned from center locations only. The map of Oregon was created by [www.maps.com](http://www.maps.com).

## 2.2 Terrestrial Laser Scanning

Terrestrial laser scanning (TLS) data was obtained using Leica ScanStation II scanner. Leica ScanStation II is a pulsed, dual-axis compensated, very-high speed laser scanner, with survey-grade accuracy, range, and field-of-view (Leica Geosystems, Switzerland). Due to high laser occlusion in forested plots the data was collected from 4 locations within the plot, center and three additional locations on the edges of the plot (see Figure 4.) Scanner was placed at 4 locations within the plot, consecutively, starting with the center scan A (Sa). Edge scan locations were placed 17 meters away from the center of the plot, where Scan B (Sb) is due magnetic north (0 degrees) from the center, Scan C (Sc) is at 120 degrees and Scan D (Sd) is placed at 240 degrees. Targets were placed 10 meters away from the center scan in locations that could be visible from all the scan locations. The center of the plot scan (scan A) was a 360 degree scan with 2 centimeter at 20 meters resolution with the dual compensator turned off. Edge scans, Sb, Sc, and Sd scanned 120 degrees looking towards the center of the plot, with 2 cm at 20 m resolution with the dual compensator turned off for time efficiency purpose (Zhang et al. 2011).

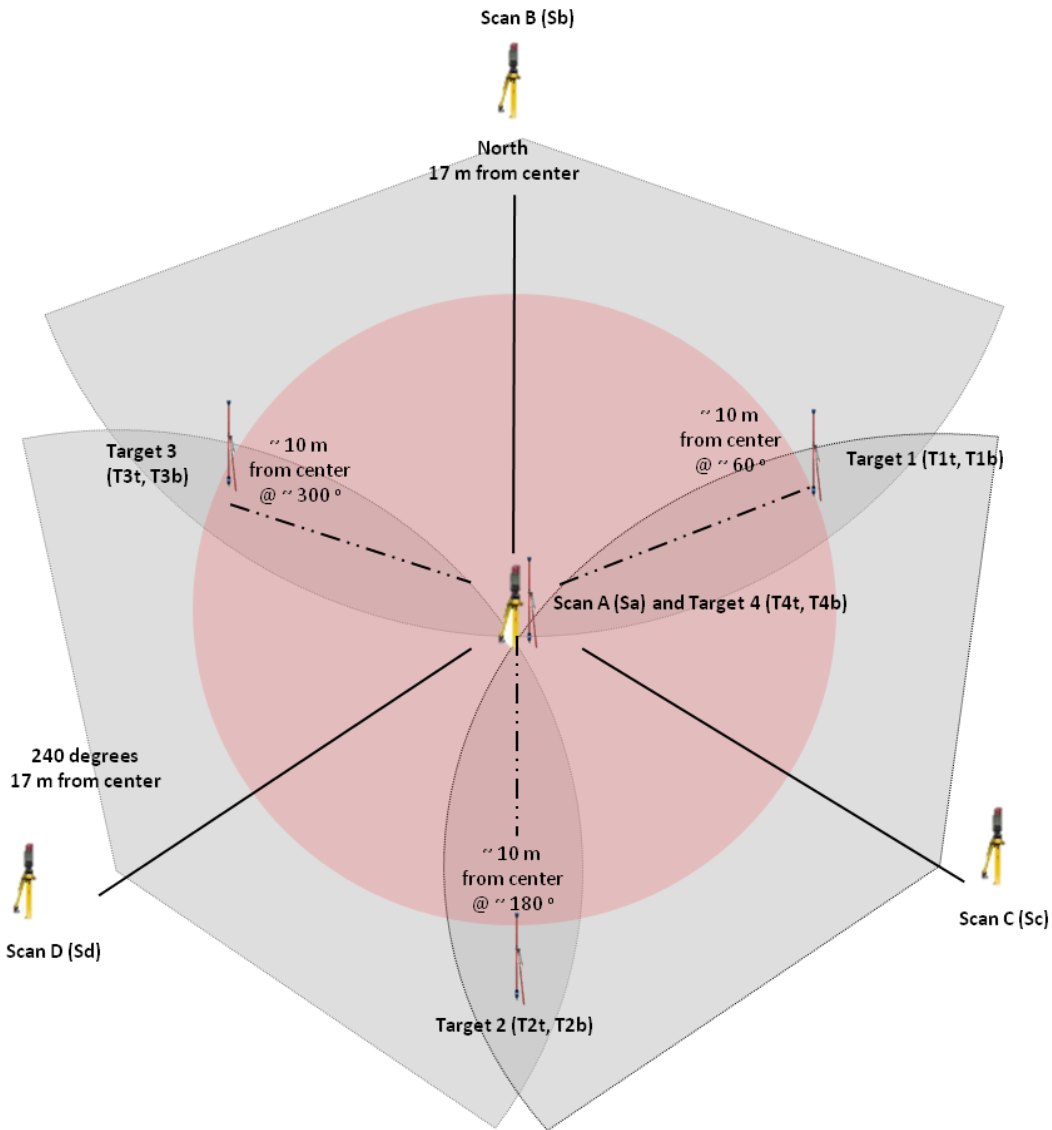


**Figure 8.** TLS scanner set up schematic for a “full scan” scanning in forested environments of dense Pacific Northwest forests. The purpose of multiple scan locations within the plot is to minimize the laser shadow effect and obtain a good 3D representation of the entire plot. (Moskal 2011, unpub.)

### 2.3 Aerial Laser Scanning

Aerial laser data was collected for the entire study area on July 15<sup>th</sup> 2010. Aerial laser scanning data was acquired using Leica ALS60 sensor mounted on Cessna Caravan 208B. The Leica ALS60 scanner was set to



acquire  $\geq 150,000$  laser pulses per second and flown 900 meters above ground level, with a scan angle of  $\pm 14$  degrees from nadir. (see Table. 1). The native pulse density over terrestrial surfaces is  $\geq 8$  pulses per square meter. Aircraft position described as x, y, and z was measured twice per second (2 Hz) by an onboard differential GPS unit. Aircraft pitch, roll and yaw were measured 200 times per second (200 Hz) from an onboard inertial measurement unit (IMU).

<b>Sensor</b>	Leica ALS60
<b>Survey Altitude (AGL)</b>	900 m
<b>Pulse Rate</b>	>105 khz
<b>Pulse Mode</b>	Single
<b>Mirror Scan Rate</b>	54 Hz
<b>Field of View</b>	28 ° ( $\pm 14^\circ$ from nadir)
<b>Roll Compensated</b>	Up to 20°
<b>Overlap</b>	100% (50% side-lap)

**Table 1.** Aerial LiDAR survey specifications (Watershed Sciences Incorporated, 2010).





**Figure 9.** Three dimensional point cloud of Panther Creek Watershed colored by RGB values from NAIP imagery. (Watershed Sciences Inc., 2010)

## 2.4 Field Data Collection

Thirty five field-based vegetation plots were established and measured during summer of 2009 and 36 additional vegetation plots were established during summer of 2010, during summer of 2011, 8 additional plots were established. During summer of 2011 46 out of earlier established vegetation plots were scanned using Terrestrial LiDAR.

## 2.5 Derivation of Variables

### 2.5.1 Terrestrial Lidar Point Cloud Processing

Raw TLS point clouds were stitched together at reference target points using Leica Cyclone software (Leica Geosystems, Switzerland). Combined point clouds for the plots were then exported in ASCII format for further processing. Fusion software (McGaughey, 2008) was used to clip the terrestrial point clouds to the 16 meter radius circular plot extent. As the Leica Scanstation 2 is a single return signal system the points that represent the ground must be filtered manually. For the purpose of digital terrain model (DTM) creation, the point cloud was further filtered to extract points that were associated with the ground. A surface model was created using the ground filtered points with 0.5 meter resolution to create a DTM. Digital terrain model represents the micro topography of each plot (see **Figure 6.**) and is further used in normalizing the height of trees and other vegetation within the plot for the changes in height due to topography.

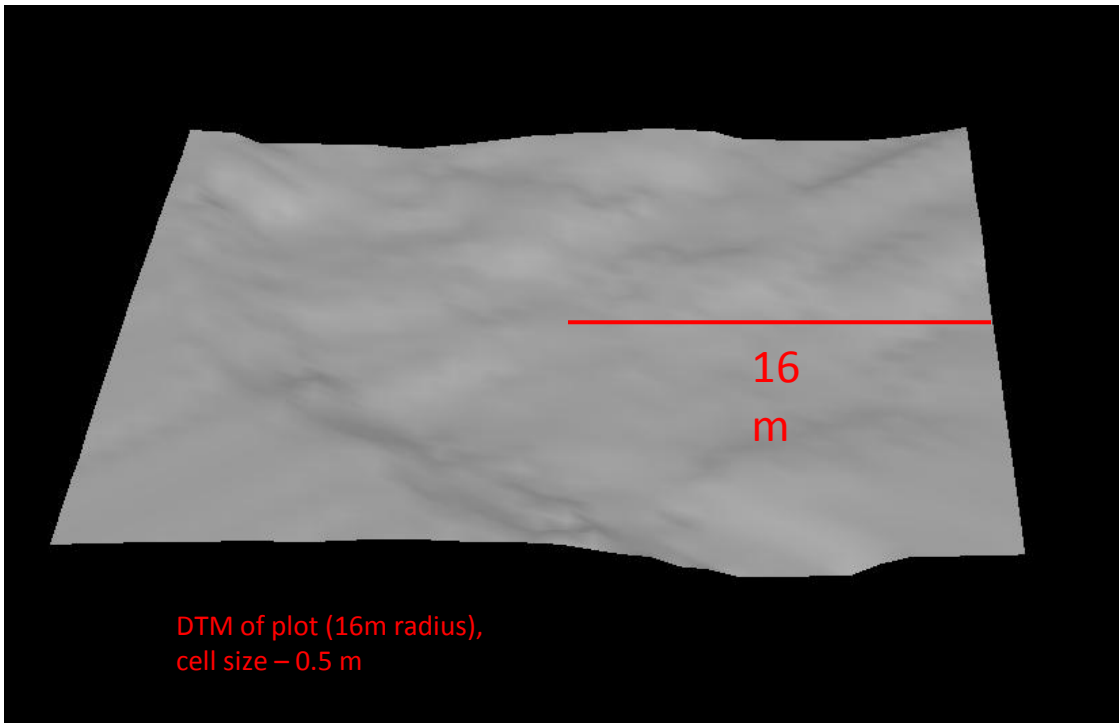


**Figure 10.** Digital terrain model of one of the study plots.

### 2.5.2 Plot Point Cloud Slicing and Canopy Surface Creation

To sample the entire plot canopy structure at various points along the vertical gradient the TLS point cloud was extracted at 6 locations throughout the canopy (see **Figure 7**). The canopy profiles were extracted at equal intervals within each plot, with first “slice” starting at the lowest height to live crown. The size of the interval varied between the plots as the plots varied in the tree height distribution. The thickness of extracted “slices” is 2 meters to make sure that the point cloud resolution is sufficient enough to accurately represent the segment of canopy at each height point (See **Figure 8**).

The canopy surface models (CSM) were then created for each canopy profile (6) for all the plots (26), totalling in 156 canopy surface models. Canopy surface models were created with Fusion software (McGaughey, 2008) using a 5 cm cell size (see **Figure 9B.5**). Such a small resolution of the CSM is necessary to accurately capture the shape, size and distribution of canopy. A smaller cell size would be preferable, however due to extremely long processing times the minimum resolution of 5 cm was chosen.

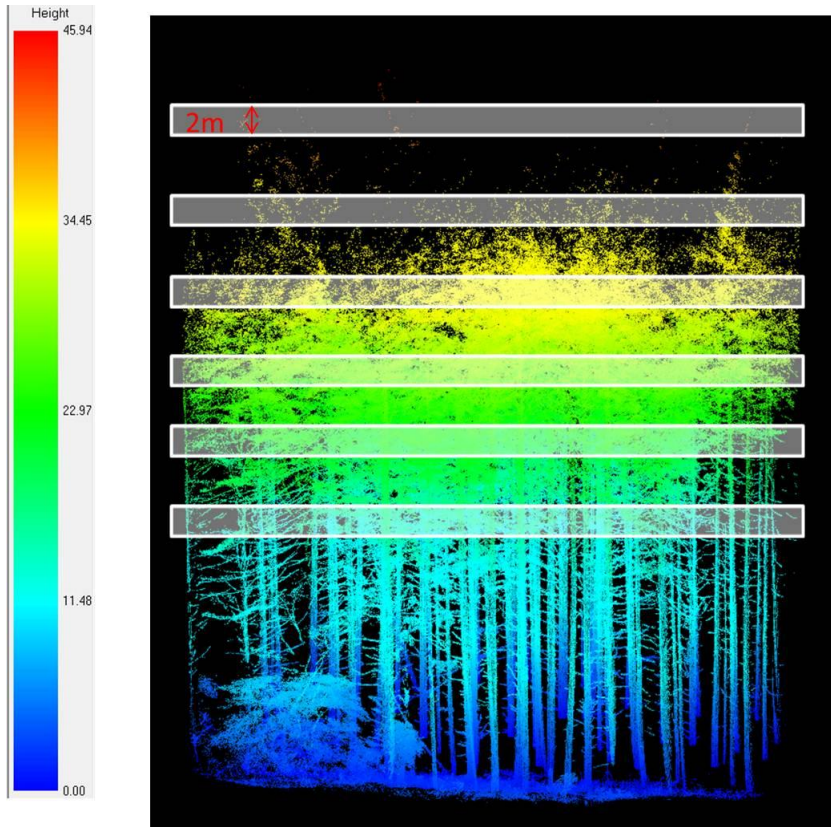


**Figure 11.** TLS point cloud slicing schematic

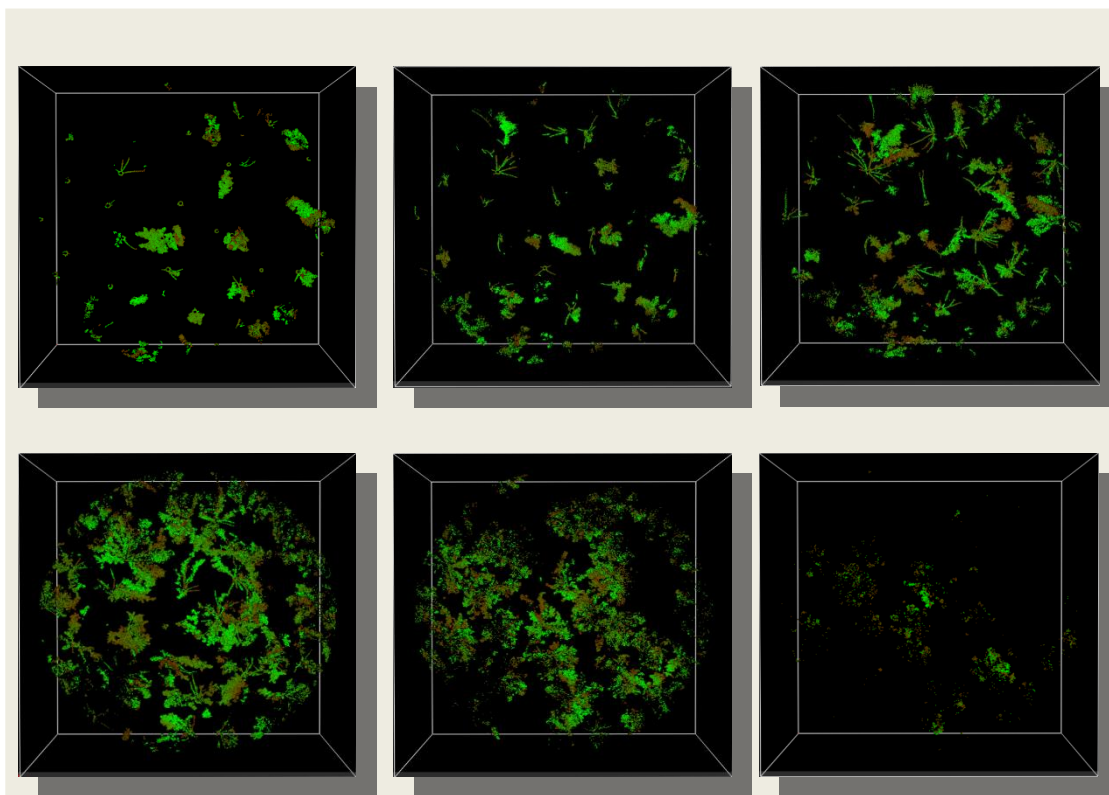


**Figure 12.** Plot TLS point cloud canopy slice: from top left to bottom right are the heights represent the lowest and the highest points of each slice for that particular plot.

### 2.5.3 Canopy Segmentation and Classification

Canopy surface models for all the canopy slices were used for canopy segmentation and classification. For this process object based image analysis (OBIA) was used. Object based image analysis is a method of classification involving delineation (segmentation) of similar pixels into discrete objects and is followed by the classification of those objects into themes or classes. An assumption of OBIA is that a landscape is made up of homogeneous patches which can be separated by their features (spectral signatures, height, texture, etc.). This analysis was performed using eCognition Developer software, which is a powerful environment for object-based image analysis, and is used in earth sciences to develop rule sets, based on algorithms, for the automatic analysis of the remote sensing data.

A surface model for each height gradient for all the study plots (n=156) were used for canopy segmentation in eCognition developer software. The segmentation algorithm used multiresolution segmentation to segment canopy surface models. For multiresolution segmentation the following parameters were used: scale parameter – 10, shape parameter – 0.5, compactness parameter – 0.5. These parameters were determined based on trial and error process and knowledge of the segmentation algorithm. The scale parameter is directly related to the size of the desired objects, with the larger number representing larger objects, the shape and compactness parameters both represent the shape of the objects, where the higher shape weights create segmentation based on shape of the objects as opposed to their spectral properties and compactness parameter represents the roundness of the objects. In this case the shape of the objects was not of much significance as we were simply separating the canopy segments from gaps. These segments were then classified into two classes: canopy and gap, the classification was based on the height information that is encoded in the surface model. All objects with NoData values were classified as Gap and objects with any kind of height information were classified as Canopy (Figure 9A.). The resulting classified objects were then merged together to create continuous patches of canopy and gaps (see Figure 9B.6). Canopy and gap polygons of canopy patches were exported as vector files into ArcGIS for further analysis.

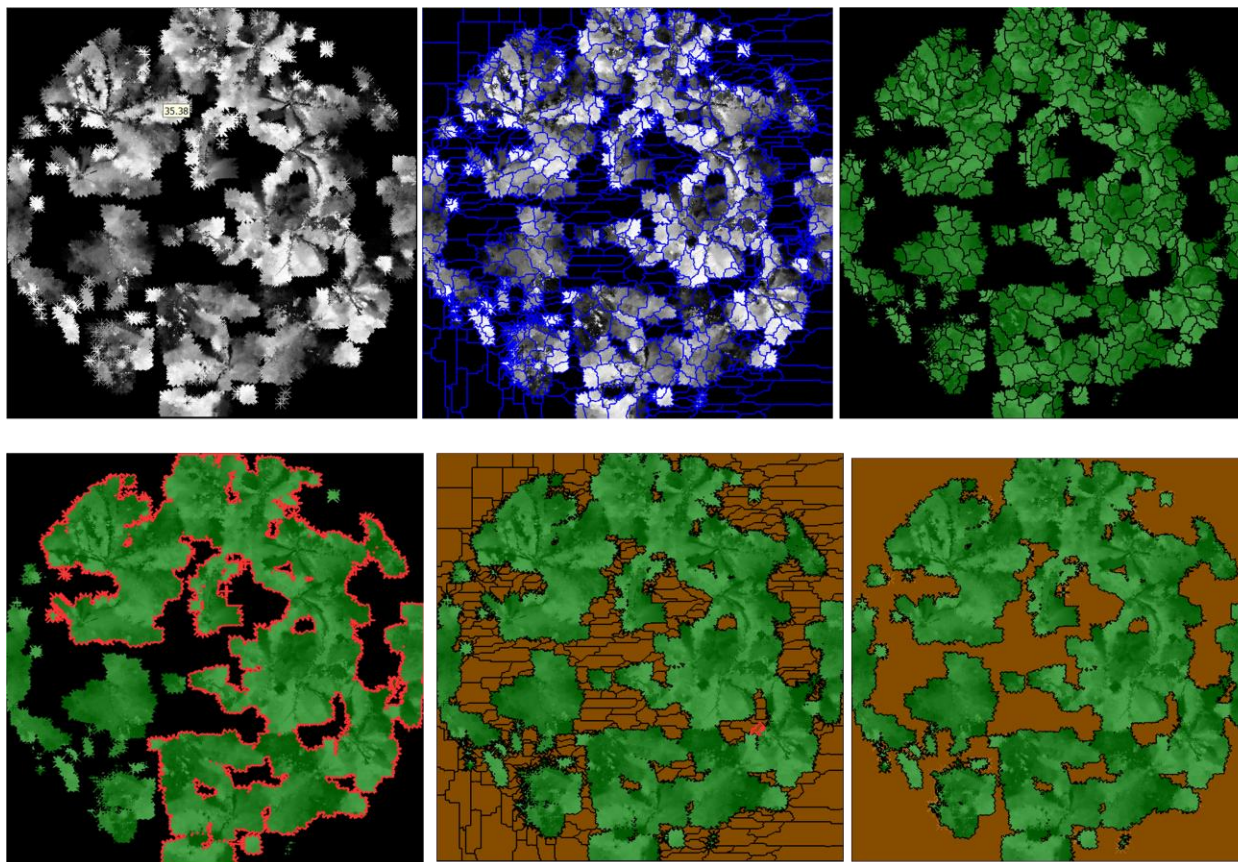


**Figure 9A.** Object based image analysis, canopy surface segmentation and classification process, where pixels (5 cm) of canopy surface (top left) created from the TLS point cloud are aggregated into meaningful objects (top middle) and resulting objects with positive height information are classified as canopy (top right). Individual objects that have been classified as canopy are then further merged to create canopy segments that represent individual canopies or multiple overlapping canopies within the plots (bottom left). After the canopy objects are merged, the remaining segments are classified as gaps (bottom middle) and objects with gap classification assigned to them are then merged together as well (bottom right).



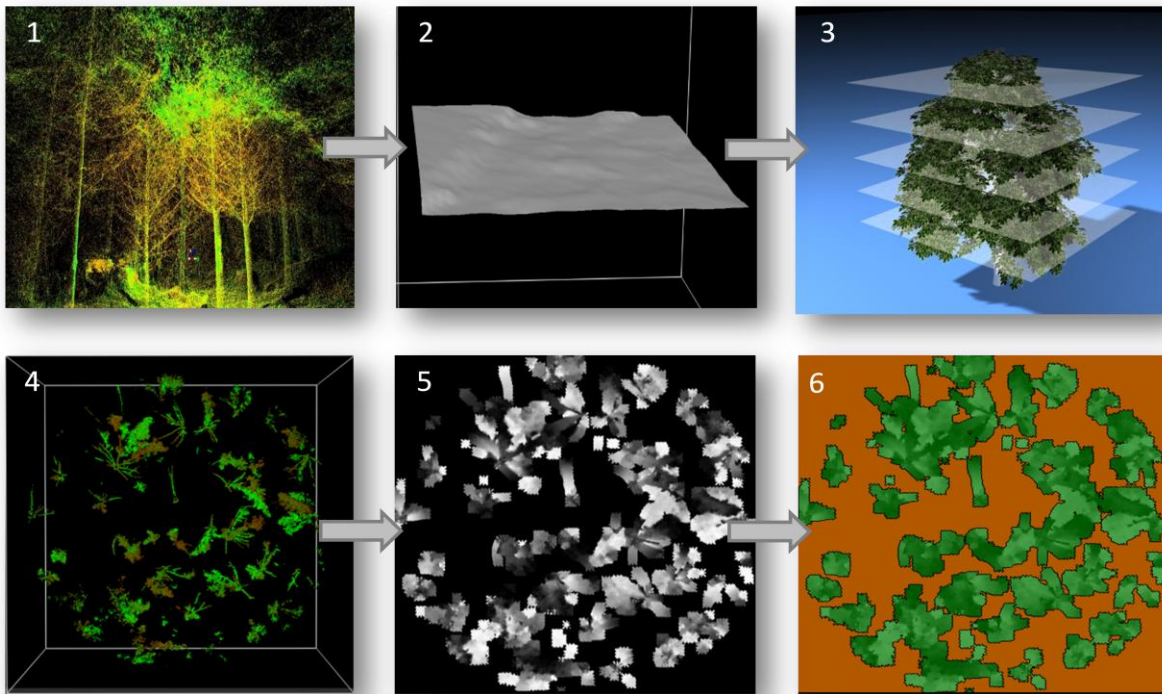


**Figure 13B.** Visual representation of the TLS point cloud processing: 1) raw point cloud of the plot; 2) DTM created by filtering ground points and creating a surface; 3) slicing the plot at six locations along the height gradient; 4) isolation of each plot's canopy slice; 5) creating a high resolution canopy surface model for each slice; 6) segmentation and classification of the canopy using OBIA.

#### 2.5.4 Extraction of Canopy Metrics

The idea behind this particular method is that once we have our spatially explicit canopy distribution maps for each study plot we can treat that canopy as a hypothetical “landscape” and extract landscape metrics from the image. The landscape metrics provide us with a way to quantitatively characterize spatial patterns of canopy structure within forest stands. The term “landscape metrics” generally is referred to indices developed for categorical map patterns. Landscape metrics are algorithms that quantify specific spatial characteristics of patches, classes of patches or landscape mosaics (McGarigal and Marks 1995). For the purposes of this research

a slightly different approach to scaling was taken. A landscape is defined as a study plot and a patch is defined as tree canopy or part of tree canopy (see Figure 10). The landscape metrics in this case were used to characterize the configuration of individual canopy patches and the distribution and density of those patches on the landscape, which in the case of this study is study plot. In use of patch metrics in describing the forest canopy structure three major components were focused on: metrics describe size and shape, patch composition and the spatial configuration of the canopy patches.

The simplest measure of configuration is patch size, which represents a fundamental attribute of the spatial character of a patch. In fact many landscape metrics either incorporate or are directly affected by the patch size. Many landscape and patch metrics exist and many of them are quite redundant. Patch shape complexity relates to geometry of patches: are they simple or complex? Regular or convoluted? Shape is extremely difficult to quantify as there are an infinite number of shapes that a patch can have, hence the shape metrics usually quantify the overall shape complexity. Commonly the shape indices are standardized to a more simple Euclidean shape as circle or square using fractal dimensions or perimeter-to-area ratios, where the higher the value of shape complexity the greater the departure from the regular Euclidean shapes. For this study mean perimeter-area ratio (MPAR) and mean patch fractal dimension (MPFD) were used. Mean perimeter-area ratio is a pretty straight forward shape complexity measure that accounts for both size and shape and number of patches on the landscape, where  $MPAR = \frac{\text{sum of each patches perimeter/area ration}}{\text{number of patches}}$ . Mean patch fractal Dimension is also a measure of shape complexity, where mean fractal dimension approaches one for shapes with simple perimeters and approaches two when the shapes are more regular.

The patch composition is referred to the landscape features associated with the variety and abundance of patch types within a landscape, without considering the location of patches within the mosaic. There are many ways to measure composition, including patch evenness, and patch diversity. For the measure of relative canopy patch diversity Shannon's Diversity Index (SDI) was used. Shannon's Diversity Index is defined as a measure



of relative patch diversity, where the index will equal zero when there is only one patch in the landscape and increases as the number of patch types or proportional distribution of canopy patch types increases. Shannon's Evenness Index (SEI) was used to measure canopy patch distribution and abundance. Shannon's Evenness Index is equal to zero when the observed patch distribution is low and approaches one when the distribution of patch types becomes more even. Please see Table 2 for a summary of canopy patch metrics used in this study; a detailed description is also available in the *List of Definitions*.

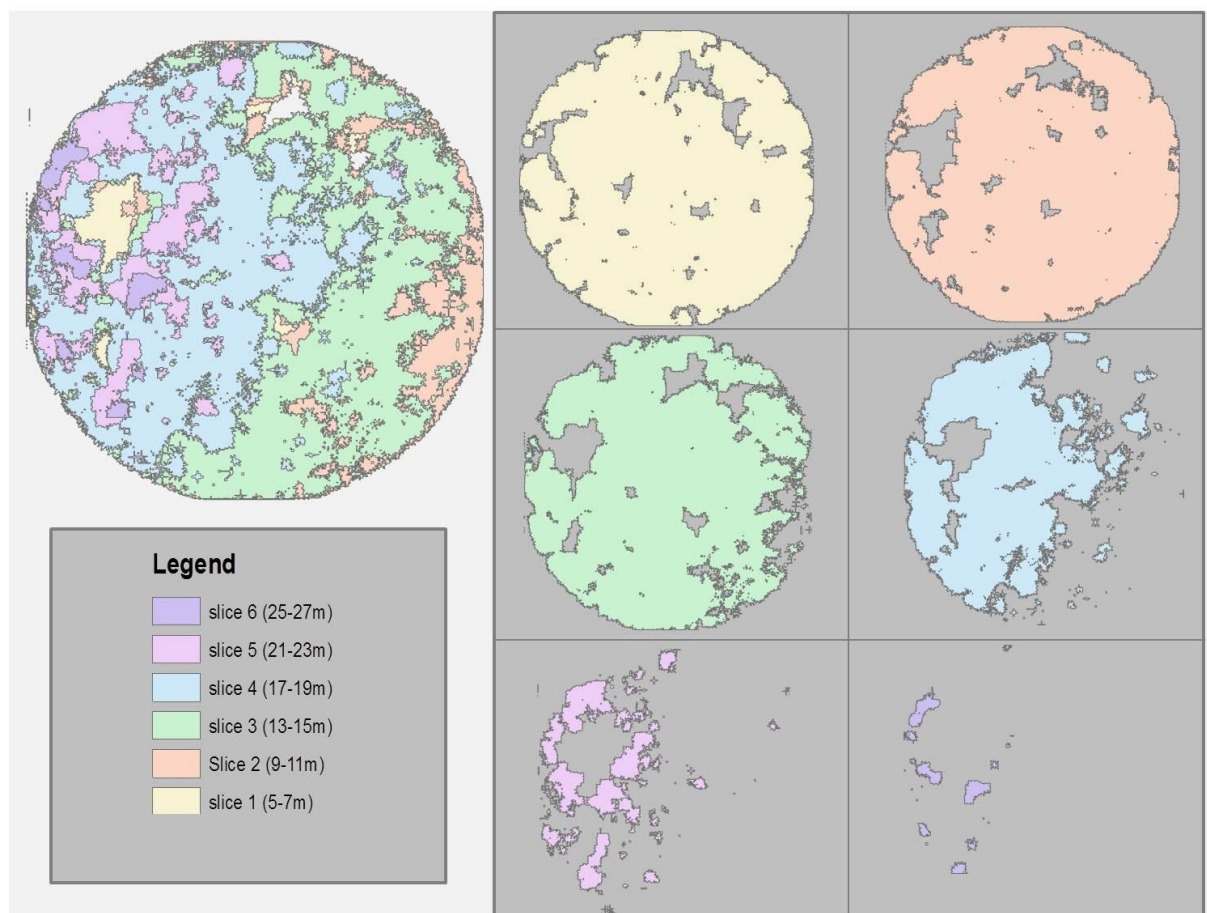


**Figure 14.** Canopy distribution maps (canopy polygons segmented and classified in eCognition) for one of the study plots

Metric Name	Description	Units
SDI	Shannon's Diversity Index	-
SEI	Shannon's Evenness Index	-
AWMSI	Area Weighted Mean Shape Index	-
MSI	Mean Shape Index	-
MPAR	Mean Perimeter to Area Ration	m/ha
MPFD	Mean Patch Fractal Dimension	-
AWMPFD	Area Weighted Mean Patch fractal Dimension	-
TE	Total Edge	M
ED	Edge Density	m/ha
MPE	Mean Patch Edge	M
MPS	Mean Patch Size	Ha
NumP	Number of Patches	-
MedPS	Median Patch Size	Ha
PSSD	Patch Size Standard Deviation	-
TLA	Total landscape Area	Ha

**Table 2.** List of patch metrics used to describe canopy structure derived from TLS point clouds. These were used to create a response variable matrix for analyses.

## 2.6 Field Plot Metrics

### 2.6.1 Density

To properly capture the variability in stand density and composition a few plot biometrics were selected. There are multiple ways to measure stand density, e.g. number of trees per unit area (trees/ha) or basal area (BA). However for the purposes of describing stand structure it is important to account for number and size of trees. Therefore stand density index (sdi) (Reineke 1933) was used to describe stand density for the purposes of this study. Reineke's sdi is a function of quadratic mean diameter and a number of trees per unit area:

$$sdi = N_o (D_o / 10)^{1.605}$$

where  $N_o$  is observed trees per unit area and  $D_o$  is the observed quadratic mean diameter.

Stand diversity index was further classified into three classes: low, medium, and high. The criteria described in Table 3. below was chosen as the classification scheme.

sdi	Type	Category
170-310	Low	1
310-448	Med	2
448-586	High	3

**Table 3.** sdi classification scheme

### 2.6.2 Composition

The study plots are dominated by Douglas fir, with a few conifer/deciduous mix plots. For the purpose of this study the plots have been classified into two stand type categories: Type I - Douglas fir, where the volume of Douglas fir exceeds 80% of the total tree volume; Type II - conifer-deciduous mix, where deciduous species such as red alder and big leaf maple are present with coniferous species such as Douglas fir, western red cedar and western hemlock. Out of 26 plots, 6 plots were classified as type II and 20 plots – type I.

### 2.6.3 Aboveground Tree Biomass and Canopy Mass

Forest biomass is a useful measure in assessing change in forest structure and estimation of carbon content, as the changes in forest biomass density is directly brought on by changes in forest structure due to natural succession, human activities, and natural impacts such as wildfire and insect damage. Biomass density is also a useful variable for comparing structural and functional attributes for forest ecosystems across a wide range of environmental conditions. Forest biomass is defined as the total amount of aboveground living organic matter expressed as oven-dry tons per unit area. For the purposes of this study aboveground biomass is defined as amount of mass stored in aboveground components of live trees and will be referred to ABG from here on.

There are multiple formulas that exist for calculating ABG. In this study species and region specific formulas were used from BIOPAK software (Standish et al., 1985)

CommonName	CODE	Biomass Equation*	Description
Douglas fir	PSME	$BAT = 37.3 + 139.3 * DBH^2 * HT$	Total Aboveground Biomass
big leaf maple	ACMA	**	***
red alder	ALRU	$BAT = 4.8 + 206.5 * (DBH)^2 * HT$	Total Aboveground Biomass
Western red cedar	THPL	$BAT = 40.4 + 96.9 * (DBH)^2 * HT$	Total Aboveground Biomass
Western hemlock	TSHE	$BAT = 29.8 + 155.8 * (DBH)^2 * HT$	Total Aboveground Biomass
grand fir	ABGR	$BAT = 30.2 + 146.9 * (DBH)^2 * HT$	Total Aboveground Biomass

**Table 4.** List of Biopak formulas used to calculate aboveground tree biomass at Panther Creek watershed

\*Total Aboveground Biomass (kg) equation using DBH (m) and Height (m).

\*\* Total Aboveground Biomass for ACMA (g) comprises of multiple equation for various parts of the tree using DBH (cm):  $BAT=BFT+BSW+BBL+BBD+BSB$

$BAT=(EXP(3.14276+1.617*LN(BDH))+EXP(3.4148+2.723*LN(DBH))+EXP(2.67176+2.43*LN(DBH))+EXP(4.7918+1.092*LN(DBH))+EXP(2.3338+2.574*LN(DBH)))$

\*\*\* BAT – Total Aboveground Biomass; BFT – Total Foliar Biomass; BSW – Stem Wood Biomass; BBL – Live Branch Biomass; BBD – Dead Branch Biomass; BSB – Stem Bark Biomass

CommonName	CODE	Biomass Equation*	Description
Douglas fir	PSME	$\ln(BCT) = 4.36933 + 2.0083 * \ln(DBH)$	Live and Dead Crown
big leaf maple	ACMA	$\ln(BCL) = 4.0543553 + 2.1505 * \ln(DBH)$	Total Live Crown
red alder	ALRU	$\ln(BCL) = 2.3429553 + 2.6232 * \ln(DBH)$	Total Live Crown
Western red cedar	THPL	$\ln(BCT) = 5.03476 + 1.8289 * \ln(DBH)$	Live and Dead Crown
Western hemlock	TSHE	$\ln(BCL) = 5.207522 + 1.7502 * \ln(DBH)$	Total Live Crown
grand fir	ABGR	$\ln(BCT) = 5.56272 + 1.6839 * \ln(DBH)$	Live and Dead Crown
Pacific madrone	ARME	$\ln(BCL) = 3.0136553 + 2.4839 * \ln(DBH)$	Total Live Crown

**Table 5.** List of Biopak formulas used to calculate canopy biomass at Panther Creek watershed.

\*The equations are based on the Biopak database. The mass is calculated in grams using diameter at breast height in centimeters.

Code	Variable	Units	Mean	StDev	Min	Max
		trees per				
Tph	trees per hectare	hectare	585.1	294.9	237.5	1337.5
plot.can.mas.kg	plot canopy mass	kg	5111.9	1735	2184.7	8621.3
qmd.cm	quadratic mean diameter	cm	39.9	14	16.4	69.1
Sdi	stand density index	-	361.4	95.6	170.4	586.3
avg.hgt.m	average height	m	28	7.3	13	48.4
avg.hlc.m	average height to live crown	m	17.6	6.1	5.3	37.1
ba.m2.ha	basal area	m <sup>2</sup> /ha	61.1	21	27.1	102.7
vol.m3	volume	m <sup>3</sup>	481	143.4	231.1	841.2
abg.t.ha	above-ground biomass	tons/ha	421.4	218.8	130.3	924.2

**Table 6.** Summary of explanatory variables used for analyses. The explanatory variables were derived from the measurements collected by the crew in the field.

Plot	Type	# of Trees	Max. Hgt (m)	AvgHT(m)	TPH(ha)	CanopyMass(kg)	QMD(cm)	sdi	BA(m <sup>2</sup> /ha)	Volume(m <sup>3</sup> )	AGB (t/ha)
104801	1	60	26.9	21.6	750	2713.9	23.6	238	33	326.7	164.5
109102	1	36	44.8	26.7	450	4187.5	37.8	304	50	386.9	336.6
200101	1	44	62.1	23.8	550	7807.1	46.5	519	93	699.5	924.2
200103	2	33	41.1	27.2	412.5	4530.9	41.7	326	56	396.7	364.4
200104	2	25	47.2	31.6	312.5	5674.8	53.1	365	69	442.0	419.4
200105	1	81	31.6	22.5	1012.5	3625.3	23.7	323	44	458.8	235.1
200106	1	38	36.2	26.2	475	3494.5	33.9	270	43	366.3	252.7
200108	1	32	44.13	35.8	400	5060.5	44.0	345	61	521.2	423.3
200109	1	21	60.7	39.5	262.5	7149.6	64.5	418	85	626.4	833.9
200110	1	19	52.6	48.4	237.5	7213.1	68.1	413	86	654.1	755.3
200111	1	34	43.1	31.8	425	5081.8	42.7	350	61	487.5	407.2
200201	1	107	41.9	25.7	1337.5	7253.6	28.9	586	87	841.2	518.2
200206	1	58	35	26.2	725	5475.8	34.1	415	66	550.1	363.7
200208	1	47	43.3	27.9	587.5	6433.0	41.8	467	80	608.9	549.9
200209	1	40	51.6	24.8	500	4108.5	35.5	305	49	389.8	341.7
200210	1	49	34.1	26.1	612.5	5085.2	35.6	376	61	435.0	354.1
200301	2	66	42.4	21.0	825	5768.9	32.7	441	69	516.1	366.2
200303	1	22	57.1	39.4	275	8621.3	69.1	490	103	652.1	917.2
200306	1	50	32.5	28.4	625	4040.7	31.5	316	49	470.1	278.5
200308	2	19	37.9	29.6	237.5	2854.0	39.2	170	29	231.1	211.5
200311	1	48	43.2	30.8	600	6120.2	39.6	437	73	624.7	503.6
200312	1	50	30.4	22.6	625	3755.2	30.4	298	45	371.4	238.0
300001	2	23	53.6	34.1	287.5	8059.2	65.5	470	96	566.0	712.8
300002	1	103	25.08	13.0	1287.5	2184.7	16.4	228	27	247.0	130.3
300005	2	38	39.4	24.2	475	4253.0	35.7	293	47	359.2	321.4
300006	1	73	30.3	18.4	912.5	3256.5	23.5	287	39	348.9	199.5

**Table 7.** Environmental variables derived from the field measurements summarized by plot.

### **2.6.4 Processing Aerial LiDAR**

Aerial lidar point clouds for the 26 study plots were extracted for the plot extent (16 meters in radius) from the raw LAS point cloud data using clipdata function in Fusion (). The clipped point clouds were then normalized by height using a 1 meter digital terrain model (DTM) provided by the vendor (Watershed Sciences Inc., Corvallis, OR). The normalized point clouds were used to extract point cloud parameters for each plot. This was done using cloudmetrics function in Fusion. The cloudmetrics output is extensive and includes metrics that describe the point cloud density, intensity, signal return break down and many others. For the list of cloud metrics used for the purposes of this study please see Appendix C.

## **2.7 Analysis**

### **2.7.1 Stand Structure from TLS**

By using the canopy metrics we can look at how the canopy structure changes with stand density, composition, and even begin looking at how aboveground tree biomass relates to stand vertical and horizontal structure. The data for this research comes from multiple sources and has taken on a multidimensional format. The first set of data are plot measurements that have been collected by crews on the ground. These data include tree heights, DBH, height to live crown, X and Y locations of each tree, etc. The second set of metrics that were used in this research was derived from the allometric measurements collected in the field (explanatory variables see **Table 6**) and were classified as the plot environmental metrics. Finally the third set of variables was estimated using the landscape metrics that from here on will be referred to as canopy metrics. These include metrics and indices that quantify canopy shape, size and distribution along a height gradient for each plot. The multidimensionality of the datasets also stems from the resolution differences. The data ranges from individual tree to plot level metrics to metrics that describe within the plot variability in canopy structure.

After the initial look at the distribution of canopy within each slice category between the plots it was clear that for some of the plots the slice 1 (at the lowest point of the canopy) had a very high point density and very high canopy patch area, which lead to believe that those were the plots with very dense and tall understory and that it was getting incorporated into the tree canopy segments. Additionally, plots with high stand density had canopy slices 5 and 6 (two top slices of the canopy) with very low point density. This can be attributed to laser's inability to penetrate through very dense tree structures. Due to the above-mentioned reasons, only slices 2, 3 and 4, that represent the middle section of the canopy height gradient were used for further analysis. For the purpose of this study the data was organized in the following fashion: The main matrix contains the patch metrics that represent shape, size, and distribution of the canopy (**Table 2.**) for 26 plots and 3 slices. The secondary matrix is a data frame that consists of plot level explanatory (environmental) variables for 26 plots; these include, but are not limited to variables that describe stand composition, density and mass (**Table 6.**)

Canopy metrics describe various characteristics of the canopy structure and come in multiple units and indices. Adjustment of data by standardizing the response variable matrix is necessary for further analysis. The data were relativized by column range, where the maximum value in a column was set to 1 and minimum value was set to 0 and all other elements were calculated as proportions between these two values. The dissimilarity matrix for the primary response variables was calculated using Euclidean distance method, because the community data in this case is derived in one way or another from various measurements of geometric distances. All following analyses were performed using R statistical software (R Core Team, Vienna, Austria, 2012).

An ordination technique helps reduce the number of dimensions while accounting for as much variability in the original dataset as possible. To combine correlated variables to reduce the dimensionality of the dataset Principal Component Analysis (PCA) was used (Craine et al. 2002; Summerville et al. 2006) using `prcomp()` function in RStudio (RStudio, 2012, Boston, MA), package `vegan` (Oksanen et al. 2012). Each



variable was scaled to unit variance, to ensure that all variables contribute equally to the results. To identify the number of principal components to use for further analysis a scree bar plot of eigenvalues was created and examined. The PCA results and the loadings for each variable were examined and interpreted for the principal components that explained the largest portion of variance.

Sums of squares multivariate regression tree analysis (SS-MRT) was used to further investigate the relationship between the canopy structure and plot characteristics and to identify the key environmental variables that drive the relationship. The SS-MRT was performed using multivariate partitioning `mvpart` and `MVPARTwrap` (Therneau et al., 2012) packages in RStudio, using the standardized matrix of response variables and raw environmental variables. The SS-MRT was run performing 100 cross-validations and 100 multiple cross-validations, using “mrt” (multivariate regression tree) method and the sum of squares were calculated using Euclidean distance (sum of squares about the mean). The size of the tree was selected manually after performing the cross validation and examining the relative and cross-validated relative errors. The tree with 3 nodes was chosen for further investigation.

To compare canopy structure between 6 slices for all the study plots PERmutational Multivariate Analysis of Variance (PerMANOVA) was used. PerMANOVA was ran with 9999 permutations using Euclidean distance measure. For data analysis statistical software RStudio, specifically `vegan` package for the multivariate analysis, was used. For the response variables first three principal components from PCA ordination were used.

To test the canopy structure differences among the canopy slices, pair-wise contrast comparisons were performed. The contrasts were tested using PerMANOVA with 9999 permutations and Euclidean method for distance measure.

To further investigate the relationship of canopy structure variability and explanatory variables an Analysis of Variance (ANOVA) was used to identify significant differences between principal components (PC1, PC2, and PC3) and the environmental variables derived from plot measurements.

To visualize the canopy metrics for all of the slices and plots a Non-metric Multidimensional Scaling (NMDS) ordination approach was used. To choose the number of dimensions the analyses were rerun with different dimensions to identify the effect of dimensionality on stress. This was done using RStudio and `vegan` package. After evaluating the NMDS Scree plot 3 dimensions were chosen (stress value=0.03), number of iterations = 9999, for the NMDS ordination. The Euclidean method for distance measure was chosen.

One of the goals of this study is to investigate the possibility of calibrating canopy structure from ALS with canopy metrics derived from terrestrial scanner point clouds. Due to the inherently different sampling density and vantage points it is important to understand what parts of the stand the two methods are sampling and how. The comparison of the point cloud distributions between the ALS and TLS was done on a subsample of the plots that represent the variability in forest structure present on the landscape, from high density, even aged, homogeneous stand to heterogeneous and low density stands. Due to the stark differences in point cloud densities the point densities (see Figure 11) within each slice had to be standardized by total number of points within the plot.

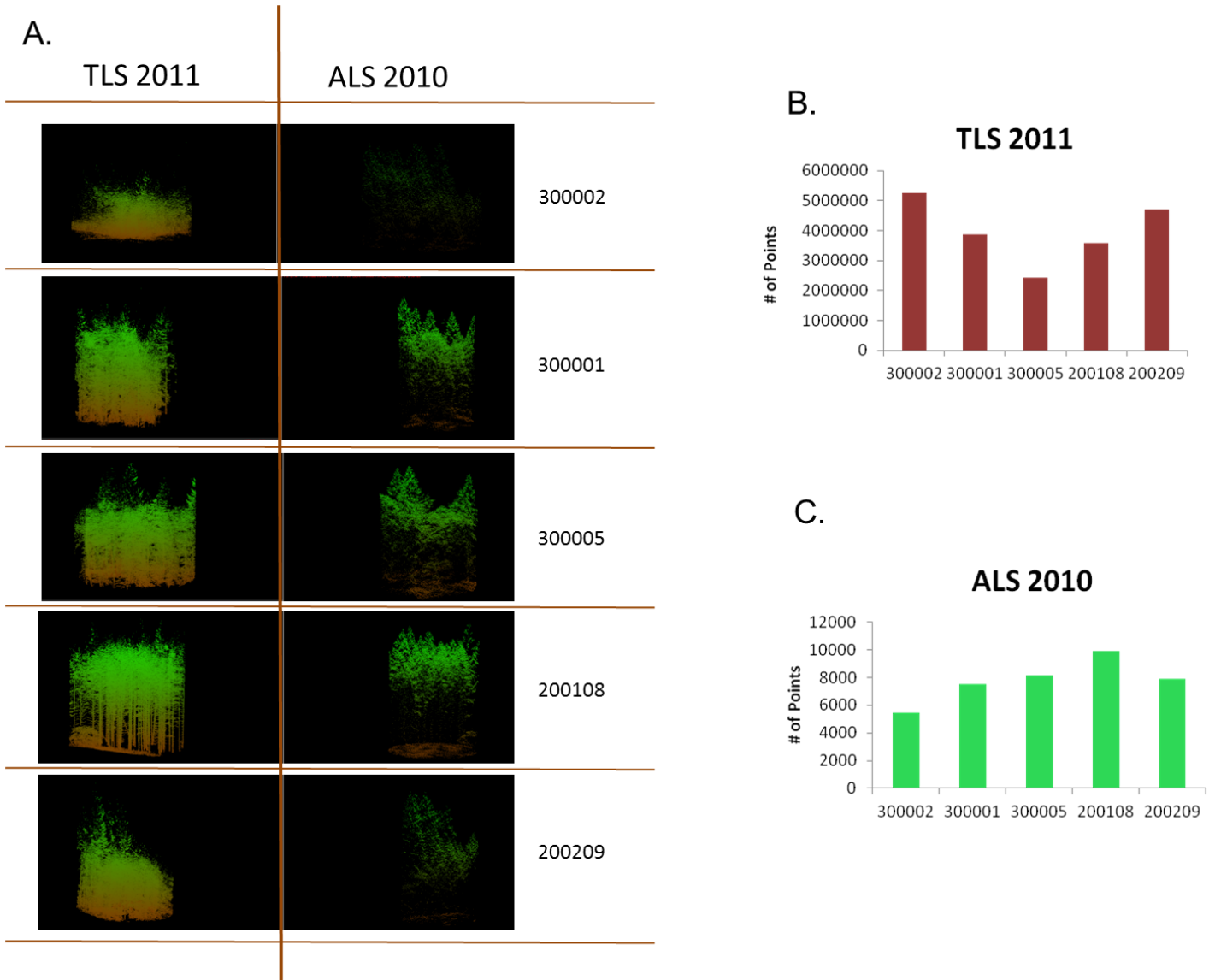


**Figure 11 A.** Differences in point cloud densities between the TLS and ALS. Raw point counts for 5 sample plots from TLS scans (**B.**) and ALS scans (**C.**)

The standardized point cloud densities from ALS and TLS for 6 canopy slices were visualized by plotting the average normalized point densities for each slice. The intersection point between ALS and TLS average point distribution was determined along the height gradient and designated as an optimum average height where the ALS and TLS data share the same amount of points, i.e. similar amount of canopy. This

approach helps eliminate the extra data layers and solely focus on the height profile where ALS and TLS intersect, which optimizes the calibration process.

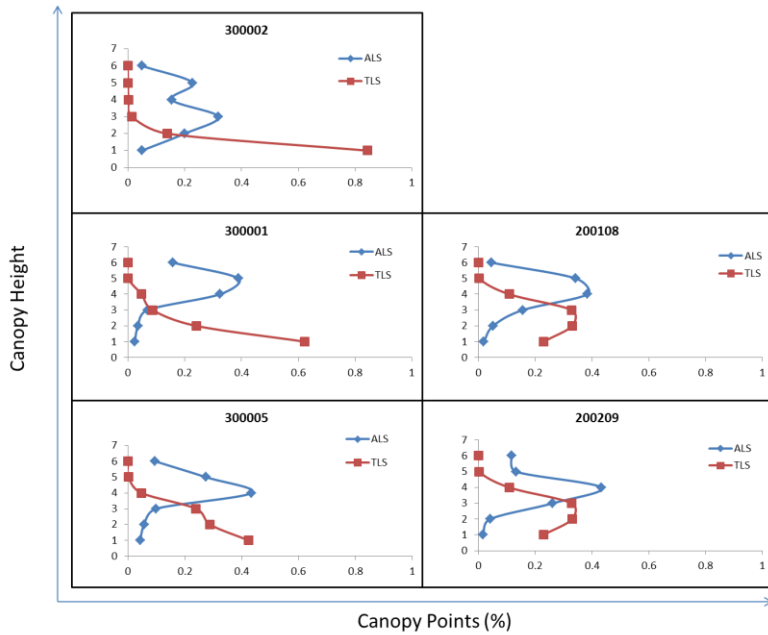


**Figure 12.** Canopy points (%) distribution along the height gradient (along the canopy slices (1-6)) for 5 example plots.

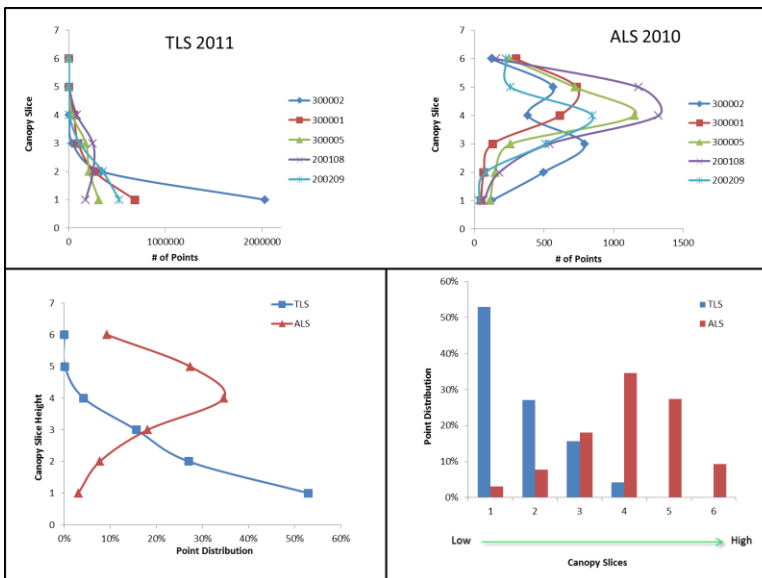


**Figure 13.** Top Left: Distribution of points for TLS example plots along the height gradient. Top Right: Distribution of points for ALS example plots along the height gradient. Bottom Left: Distribution of TLS points for averaged ALS and TLS plots along the height gradient. Bottom Right: Point distribution for ALS and TLS point clouds for each slice along the canopy (1-6, low-high).

Two approaches were tested for calibration of ALS with TLS data sets. The first approach followed the methodology described in TLS processing and canopy metrics extraction and extracted the ALS point clouds at exactly the same locations along the canopy as the TLS slices. The resulting ALS derived canopy metrics were then compared to TLS derived canopy metrics and field derived plot metrics. The second approach, took into consideration the considerable differences in point cloud density between the two scanning methods. Instead of creating spatially explicit canopy patches from ALS derived point clouds, metrics directly related to the ALS point cloud were used (please see Appendix C., list of Cloudmetrics). These metrics represent point cloud statistics and incorporate height, return and intensity information for a given area. Out of a multitude of metrics only a few were chosen for the model building approach. These metrics were chosen based on their relevance to the canopy structure metrics, and are focused on the point cloud statistics that are related to percent returns for certain height statistics.

### **3. Results**

Although for this research the focus was predominantly on canopy structure of the stands, the method described in this study can be applied to describe many other spatial distributions within the plot. The slicing and surface creating method accurately captures the spatial distribution of stand parts and quantitatively characterizes the attributes of the stand features on any desirable height gradient with any desirable sampling frequency. One can omit the canopy and slice the stand at the lower height gradients from ground to crown to capture the volume and distribution of understory within the plot. This kind of understory mass quantification is

a superior approach to the current method of vegetation transects or sampling square meter subplots that sample a very small part of the plot and then are further extrapolated to the rest of the surface.

After examining the results of PCA scree plot (**Figure 14**) it appears logical to focus on the first three components. There appears to be a break in the scree plot, where each of these eigenvalues is greater than the mean eigenvalue, and together they explain 83% of the variance.

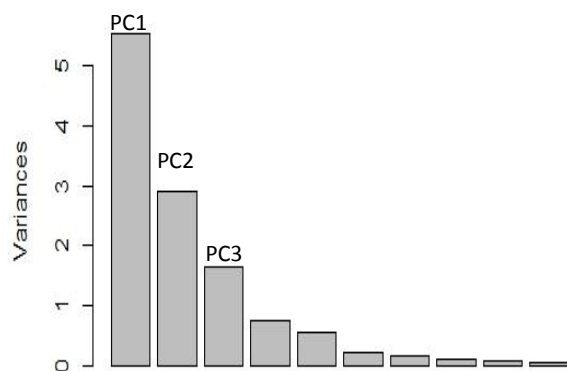


**Figure 14.** Scree plot of principal component analysis (PCA), where first three principal components explain 82.8% of variability in the canopy structure metrics.

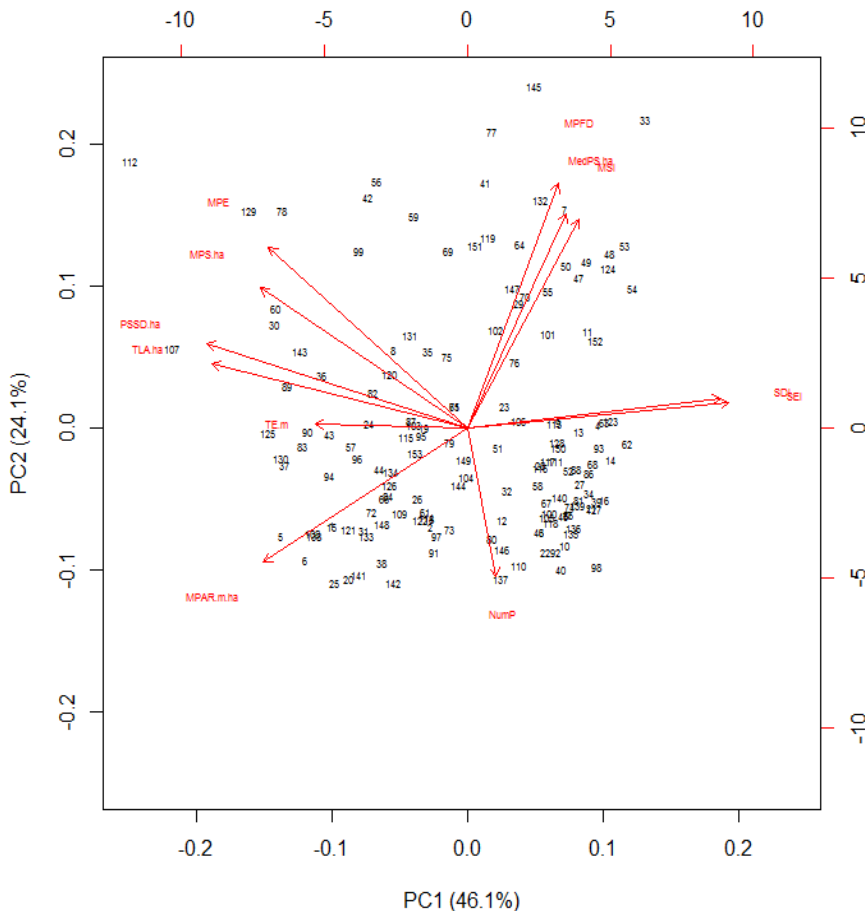


**Figure 15.** PCA Ordination, where PC1 and PC2 are the axes, and the eigenvectors represent the canopy patch metrics used as response variables.

After examining the magnitude and directions of loadings for PC1 (**Table 8**) it can be concluded that SDI and SEI, as well as the canopy patch size standard deviation (PSSD.ha) and total canopy area (TLA.ha) are given somewhat equally bigger weights it therefore can be concluded that PC1 can be interpreted as a measure of canopy distribution (diversity and evenness) and canopy size (patch size standard deviation and total canopy size). The loadings for PC2 give the most weight to a canopy metric MPFD (mean patch fractal dimension) and MSI (mean shape index) and can be interpreted as a measure of canopy patch shape complexity. The loadings for the third principal component (PC3) indicate that it can be interpreted as the canopy patch total edge metric (TE.ha) and total number of canopy metrics (NumP) (**Table 8**).

	PC1	PC2	PC3	
Distrib.	SDI	0.371	-0.026	0.118
	SEI	0.371	-0.051	0.085
Shape.	AWMSI	-0.178	0.340	-0.293
	MPAR.m.ha	-0.318	-0.038	0.294
	MPFD	0.296	-0.191	-0.202
Edge	AWMPFD	-0.046	0.028	-0.523
	TE.m	-0.123	0.339	-0.368
	ED.m.ha	0.202	0.299	0.094
	MPE	-0.162	-0.271	-0.374
Size	MPS.ha	-0.205	-0.335	0.076
	NumP	0.053	0.431	0.130
	MedPS.ha	0.261	-0.129	-0.130
	PSSD.ha	-0.306	-0.258	0.045
	TLA.ha	-0.350	-0.128	-0.047
<b>St.Dev.</b>	2.5929	2.1683	1.3544	
<b>Prop.of.Var</b>	0.4202	0.2938	0.1147	
<b>Cum.Prop</b>	0.4202	0.714	0.8287	

**Table 8.** First three Principal Components (PC1, PC2, and PC3), and the loadings of each component for the response variables, here represented by the canopy patch metrics. Highlighted are the loadings for the variables that were used to further interpret the principal components. **PC1** - canopy patch distribution and size; **PC2** – canopy patch shape and number of patches; **PC3** – canopy patches edge length and edge complexity

Sums of squares multivariate regression tree analysis (SS-MRT) was used to further investigate the relationship between the canopy structure and plot characteristics and to identify the key environmental variables that drive the relationship. The fit of the tree was assessed using the complexity parameter (cp), and cross-validated relative error (CV Error=0.8). The splits at the top of the tree are more important than variables that are invoked lower in the tree (**Figure 16**). At the first node (starting number of observations = 77), the split was made at aboveground biomass, however these were the primary splits: aboveground biomass (t/ha) with cp=0.199, volume of trees (m<sup>3</sup>), cp=0.176, average tree height (m), cp=0.159, number of trees per plot, cp=0.149, and trees per hectare, cp=0.149. The largest percent contributions of each canopy metric to the first



node are summarized here in descending order: SEI- 19.1%, SDI – 16.4%, MPFD – 11.7%, MedPS (ha) – 10.9%, PSCoV – 10.7%, and TLA(ha) – 7.7%.

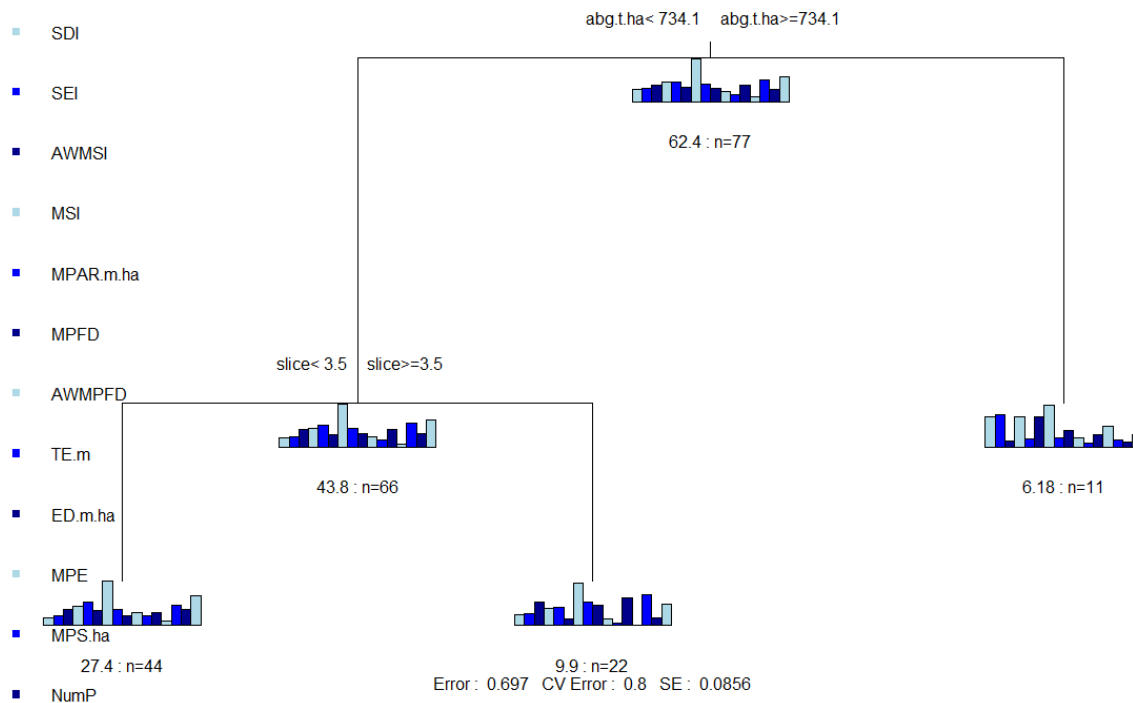


**Figure 16.** Multivariate Regression Tree, separating the field measured explanatory variables. The tree was created with 3 nodes using the complexity parameter and cross validation error to assess the fit. For the list of metrics in the legend please see Table.1.

The second node started with 66 observations and was made using canopy slices, these were the other primary splits for the second node: slice,  $cp=0.147$ , quadratic mean diameter (cm),  $cp=0.06$ , aboveground tree biomass (t/ha),  $cp=0.06$ , average tree height (m),  $cp=0.06$ . These are the largest contributing canopy metrics for the second node of the regression tree: NumP – 23.3%, ED – 12.2%, PSCoV – 11.3%, TLS – 8.5%, PSSD – 7.6%, and MPFD – 7.6%. The cross validation error (CV error) for the multivariate regression tree is 0.8; relative error is 0.69, and standard error (SE):0.085.

The attempts to find differences in canopy structure between all the canopy slices (6) using a PERMANOVA test were not statistically significant. The most likely reason for this is the fact that we have

used all the height slices together for the analysis, and as an observation, it has been noticed that some of the lower canopy slices (1 and 2) incorporated points from understory in them. Additionally, in the more dense plots, the top two slices (5 and 6) were significantly underestimating the amount of canopy present at those height gradients; this is due to high density of stands occluding the path of the laser from penetrating into the higher canopy layers. As a result, it has been concluded that for the analysis purposes only gradient layers 3 and 4 will be used for analysis of variance.

Permutational multivariate analysis of variance has shown that the canopy structure significantly ( $\text{pseudo-F}_{(2,74)} = 6.0032$ ,  $p < 0.0001$ ) varies between the canopy slices along a stand height gradient. Further testing the canopy structure differences among the canopy slices using pair-wise contrast comparisons revealed that slices 2 and 3 were not statistically significantly different from each other, however slices 3 and 4 ( $\text{pseudo-F}_{(1,74)} = 6.36$ ,  $p = 0.001$ ) and slices 2 and 4 ( $\text{pseudo-F}_{(1,74)} = 9.35$ ,  $p = 0.0002$ ) significantly varied between each other (**Figure 17**).

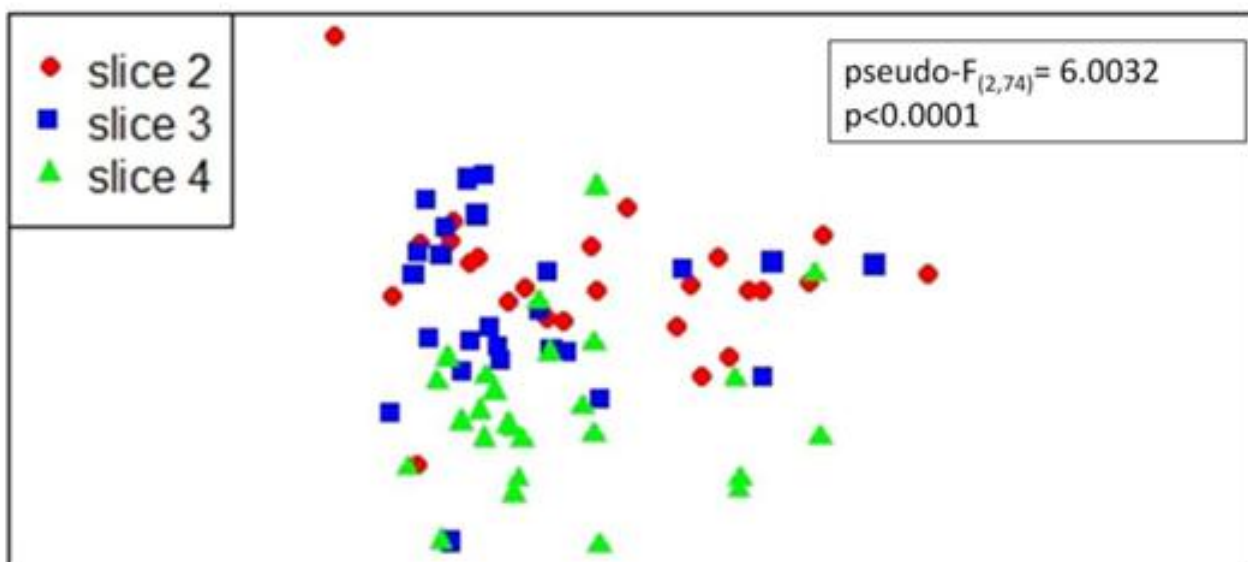


**Figure 17.** NMDS ordination of plot canopy structure metrics by canopy slice, where slice 2, 3, and 4 represent height gradients from low, medium and high, respectively. The ordination was run using 3 dimensions, with stress value of 0.03, it was iterated 9999 times, using Euclidean distance measure. The statistics show the significance of the canopy structure difference between the slices.

There were no significant statistical differences in canopy structure between plots with varying composition. Perhaps the grouping of the plots in only two types has created a very coarse separation that did not allow the detection of statistically significant differences. The other reason for this result is the great difference in the sample numbers for each category, where Type I category (n=20) is a Douglas fir dominated stand and Type II category (n=6) is represented by mixed stands. Perhaps a much more sensitive discrimination between the stand types or species richness or a diversity index will allow for greater sensitivity in the analysis of variance detecting differences in canopy structure between plots of varying stand compositions. Additionally for better results separating the differences in canopy structure between the plots with variable species composition a matrix of species abundance should be used as an explanatory matrix, this particular approach will allow to assess the tree species community composition effects on the canopy structure.

Stand structural characteristics, specifically, aboveground tree biomass (t/ha), quadratic mean diameter (cm), average height to live crown (m), average tree height (m), basal area (m<sup>2</sup>/ha) and stand density index were all significant predictors of stand canopy structure summarized in first three principal components (PC1, PC2 and PC3). (**Table 9**).

EnvVariable	df	Res df	R <sup>2</sup>	Pseudo-F	p-value
slice	1	151	0.22	42.77	<b>0.0001***</b>
plot	1	151	0.0003	0.047	0.98
st.type	1	151	0.003	0.45	0.706
tph	1	151	0.015	2.3	0.081
<b>abg.t.ha</b>	1	151	0.036	5.65	<b>0.0032**</b>
plot.can.mas.kg	1	151	0.025	3.87	0.014*
<b>qmd.cm</b>	1	151	0.031	4.83	<b>0.0055**</b>
sdi	1	151	0.014	2.13	0.1
<b>avg.hgt.m</b>	1	151	0.032	5.04	<b>0.0045**</b>
<b>avg.hlc.m</b>	1	151	0.032	5.05	<b>0.0039**</b>
ba.m2.ha	1	151	0.023	3.58	0.0206*
vol.m3	1	151	0.022	3.32	0.0277*

**Table 9.** PerMANOVA results, where the response variable matrix consists of first three principal components and the explanatory variables can be looked up in the Table.

Canopy metrics composition had a linear positive correlation with aboveground tree biomass (t/ha) (pseudo- $F_{(1,75)} = 13.8$ ,  $p = 0.0001$ ), and where the stand density index had a less of an effect on the variability in canopy structure (pseudo- $F_{(1,75)} = 3.8$ ,  $p = 0.015$ ) (**Figure 18**).

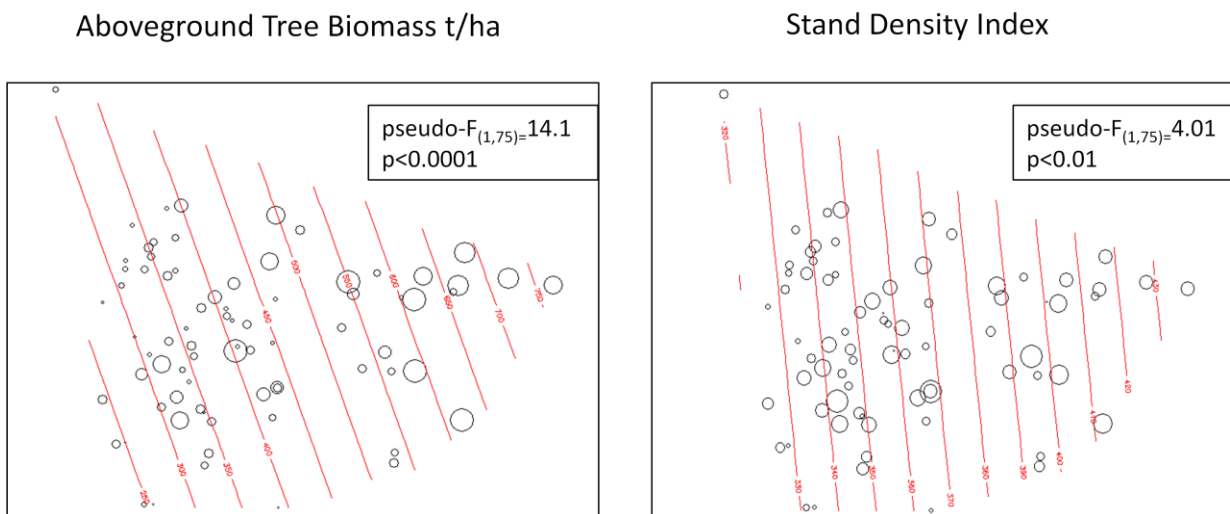


**Figure 18.A** NMDS ordination of canopy structure metrics linearly correlated with aboveground tree biomass (t/ha) and the PerMANOVA results showing a significant effect of aboveground tree biomass (t/ha) on canopy

structure. **B.** The NMDS ordination showing the effect of Stand Density Index (SDI) on the plot level canopy structure derived from TLS point cloud.

Direct tree measurements such as height and height to live crown and diameter had a highly significant effect on variability of canopy structure. The PerMANOVA results are summarized in the **Table 10**.

	Slice	Plot	St.Type	TPH	ABG	QMD	SDI	Avg.hgt	Avg.HLC	BA	Volume
3PCs	***	***		**	***	***	*	***	***	***	**
PC1		**		*	***	***	*	**	***	**	**
PC2	***			**		*		**	**		
PC3		***					*			*	*

**Table 10.** PerMANOVA and ANOVA results, significance levels, where **PC1** can be interpreted as canopy patch distribution and size, **PC2** – canopy patch shape and number of patches, **PC3** – canopy patches edge length and edge complexity

After examining the results of ANOVAs, it can be concluded that aboveground tree biomass ( $F_{(1,75)}=27.37, p=0.0001$ ), quadratic mean diameter (cm) ( $F_{(1,75)}=15.22, p=0.0004$ ) and height to live crown ( $F_{(1,75)}=14.03, p=0.0005$ ) had a significant effect on canopy size and distribution (PC1). Canopy patch shape and total number of patches within slice (PC2) varied significantly with variability in trees per hectare ( $F_{(1,75)}=8.07, p=0.006$ ) and average tree height (m) ( $F_{(1,75)}=10.64, p=0.0014$ ). Basal area (m<sup>2</sup>/ha) ( $F_{(1,75)}=6.11, p=0.015$ ), stand volume (m<sup>3</sup>) ( $F_{(1,75)}=4.6, p=0.034$ ) and stand density index ( $F_{(1,75)}=5.9, p=0.018$ ) significantly affected the canopy patch edge length and edge complexity (PC3).

Canopy structure metrics derived from TLS and ALS slices were used in attempt to find a connection between the two sources of remotely sensed data. The lack of any overlap and significant relationship between the two datasets (**Figure 19**) is most likely coming from the disparity in the point cloud density, where the

canopy surfaces created from ALS point clouds are significantly smaller and more disconnected, making it very difficult to directly compare the canopy structure derived from two datasets.

### Canopy Structure Metrics NMDS

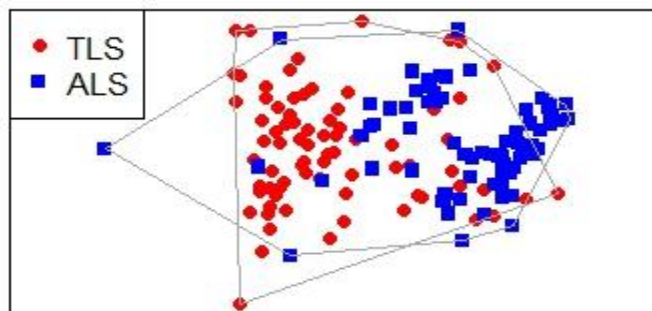


**Figure 19.** NMDS ordination of canopy structure metrics for ALS and TLS derived canopy patches, it shows very little overlap between the two and indicates the fact that a different approach to comparing the canopy structure between two data sources is needed.

Such disconnect in the point cloud density has prompted a different approach to calibration of ALS with TLS point clouds. Instead of directly comparing the canopy distributions between the two datasets, statistical metrics from ALS point cloud data were used to summarize the plot canopy instead and directly related to TLS derived canopy structure metrics. Stepwise regression model building approach was used to relate the ALS derived cloudmetrics to canopy structure metrics grouped into principal components that describe the canopy size, shape and canopy patch spatial distribution (see Table 8). As a result two simple models emerged from this approach. Where PC1, or canopy patch distribution and size, and PC2, canopy patch shape and number of

patches, are best described by linear models that are the combinations of percent 3<sup>rd</sup> and 4<sup>th</sup> returns. Here are the final models that can be used to calibrate aerial lidar with canopy metrics derived from TLS:

$$PC1 = 19.837 * \% \text{ of } 3^{\text{rd}} \text{ returns} + 1500.17 * \% \text{ of } 4^{\text{th}} \text{ returns} - 3.798$$

$$PC2 = 124.6858 * \% \text{ of } 3^{\text{rd}} \text{ returns} + 560.6342 * \% \text{ of } 4^{\text{th}} \text{ returns} - 2.7312$$

The models above indicate that the number of 3<sup>rd</sup> and 4<sup>th</sup> returns are best at describing canopy structure, as those are the returns of laser signals that penetrate through the canopy and reflect back from the branches within the canopies and off of the subdominant trees that are not otherwise picked up by the first returns. First returns are usually used to create canopy surface models and according to the findings above they typically exclude the interior canopy structure and structure of complex multi-layered canopies of the Pacific Northwest forest stands.

#### **4. Discussion**

Spatial canopy structure of Pacific Northwest forests provides key information about the biomass accumulation and distribution, its contribution to biogeochemical cycling and tree physiological function. It is difficult to measure canopy structure and verify the accuracy of the measurements. Most of the methods previously used in the field require estimates derived from allometric relationships derived from DBH and height, or canopy parameters directly collected by the laser range finders. Canopy structure has also been previously described using LAI and gap fraction analysis. It is also challenging to test the accuracy of the canopy structure derived from TLS. In this study I have tested the use of the terrestrial LiDAR for spatially explicit collection of canopy structure parameters. Structure derived from TLS was tested using structure components derived from field measurements. Both methods have uncertainty associated with them, field measurements are prone to human measurement and instrument error and TLS is very susceptible to stand density, both understory and overstory. Plots with dense and tall understory were problematic as the laser beam

was obstructed by the lower understory vegetation, especially at the larger scan angles. Plots with high tree density had very poor laser penetration into the higher canopy, as the laser was intercepted by the very dense, thicket like, young stands. Terrestrial LiDAR is more effective at capturing canopy structure in lower density, low understory, older, vertically and horizontally diversified stands. The laser beam was able to capture the canopies of individual trees and the distribution of canopy within the plot at various heights along the vertical gradient. The lower the plot density the more accurate the point cloud representing the canopy structure.

Stand density can also be derived from the TLS structure. The canopy point cloud can be extracted from a mid-point in the canopy and canopy metrics that indicate the size, shape and distribution vary significantly between plots with varying density (Figure 20.). It is important to note that if canopy structure is extracted from lower or higher canopy the accuracy significantly reduces, where the lower canopy may incorporate tall understory and high canopy is not well represented in the dense plots due to poor laser beam penetration through the dense and overlapping branch arrangement.



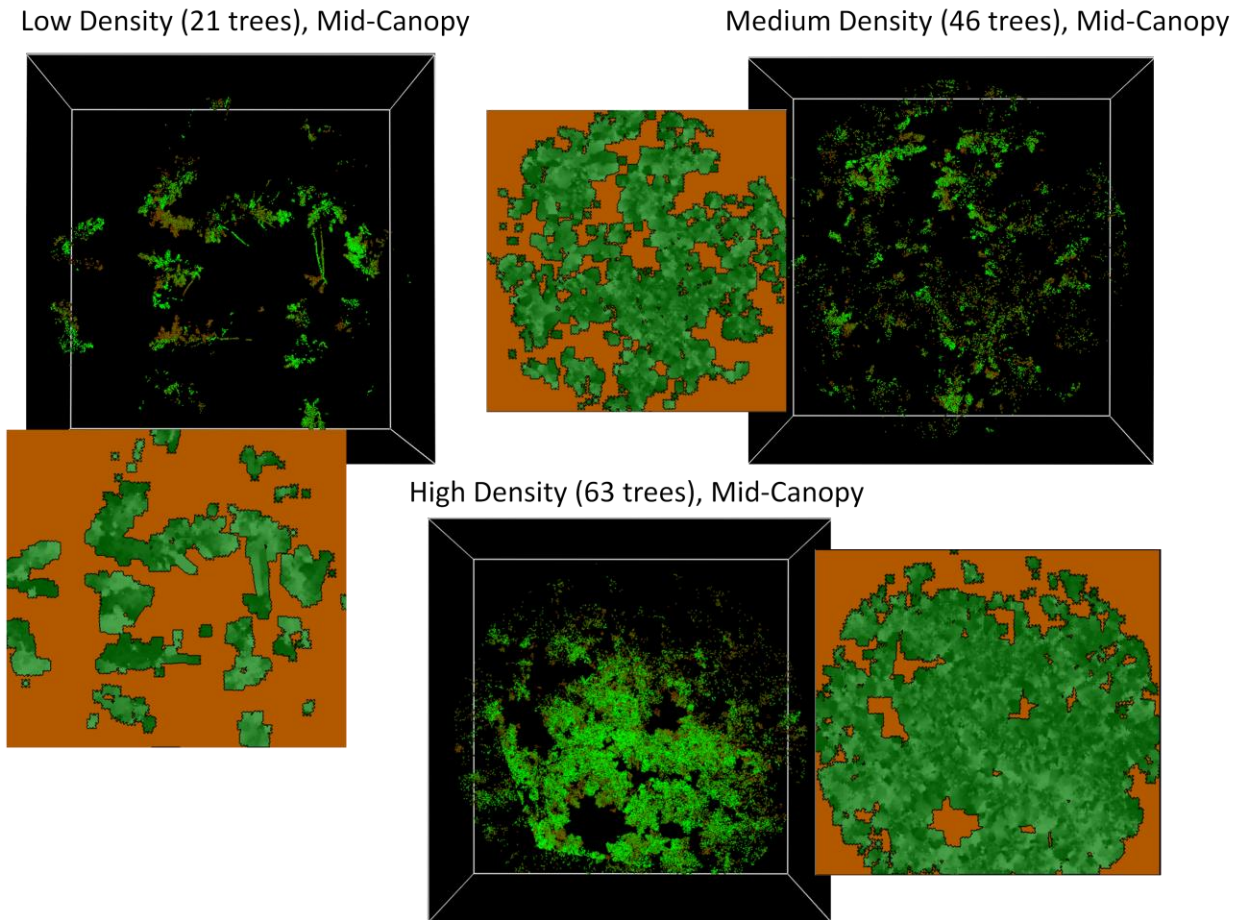
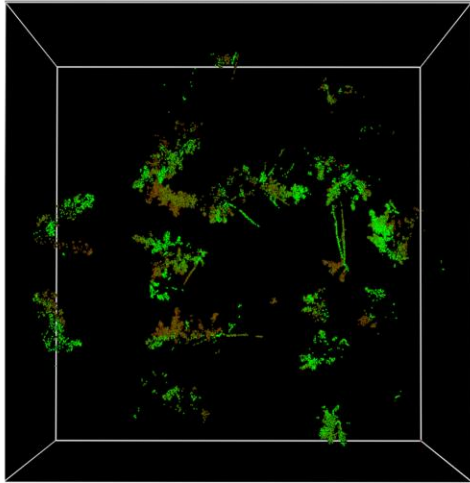


**Figure 20.** The graphic shows mid-canopy slices of three distinctive plots in respect to the tree density. The images with black background represent segments of the raw point clouds from TLS and images with orange background represent the respective canopy distribution maps generated from the point clouds, where green represents canopy patches and gaps are colored in orange.

Plot species composition is an important factor in canopy structure composition, where the plots with deciduous species have a much more connected canopy with higher total canopy area, and monoculture conifer plots had canopy with a greater number of smaller patches that were spaced evenly within the plot with higher gap areas in between. Even though we can visually distinguish the differences between deciduous/mixed and conifer plots (Figure 21.), statistically the differences in canopy structure metrics were not significant. This is attributed to a very low sample size of deciduous/mixed plots.

- **Conifer**
- 22 trees
- Mid canopy



- **Deciduous**
- 21 trees
- Mid canopy

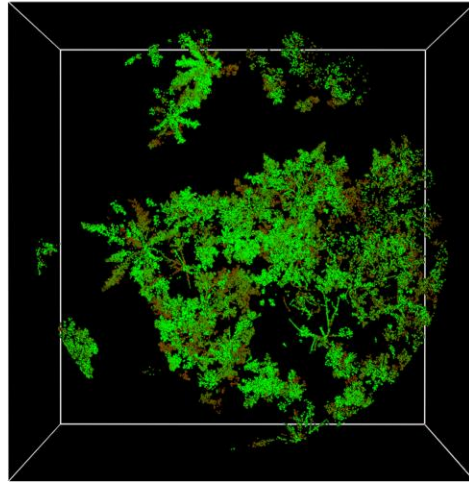


**Figure 21.** Raw point clouds for mid-canopy slices for two plots with similar densities but different compositions, conifer plot on the left and deciduous/mixed plot on the left.

#### *Connecting TLS with ALS*

One of the goals of this study was to investigate the potential of calibrating the laser point clouds with data obtained from terrestrial laser scanning. Plotting the average point distributions for both terrestrial and aerial lidar showed that the two datasets intersect at slice 3 and 4. Those are located in the mid canopy and canopy structure within mid canopy was further used as the ultimate point of comparison. After testing multiple approaches, it has been determined that directly comparing the canopy distribution obtained using identical method from both TLS and ALS does not work due to the significant differences in point cloud densities between the two data sources. A method that involves canopy metrics derived from spatially distributed “landscape” metrics from TLS and point cloud metrics from ALS, “cloudmetrics”, is a better approach. This derivation of canopy structure parameters can be considered independent and the differences between the point cloud densities are accounted for as both are standardized by the total number of points.

As the result of model building approach it has been determined that the percent of third and fourth returns is best for predicting canopy structure. Third and fourth returns represent the returns from the laser pulses that have penetrated through the top of the canopy and are now reflecting from the structure within the canopy. Fourth returns are generally considered ground points, however in dense forested stands fourth returns reflect from within the canopy instead of hitting the ground. This result indicates that most commonly filtered out of the analysis third and fourth returns provide very valuable information about canopy structure of vertically and horizontally complex forests over large areas.

#### **4.1 Sources of Error**

As with any laser terrestrial based sensor occlusion or laser shadow is a significant source of error, even though for this research project we tried to eliminate as much of the occlusion error as possible by scanning from multiple vantage points within each plot and then stitching the scans together, there is still an issue with an accurate representation of the plot in denser stands.

The need to obtain the scans from multiple locations within the plot also introduces a minor error within the process of stitching the scans together, generally the error associated with stitching is sub-centimeter and does not significantly impact the results of this study.

Weather condition during point cloud collection can impact the accuracy of the point cloud and it's ability to accurately capture the three-dimensional structure of the canopy. The biggest issue arises with windy conditions that cause the canopy to move and therefore result in "fuzzier" scans. This can lead in a wider distribution of laser points and overestimate the canopy surface. It is important to make sure that data collection is taking place during favorable weather conditions with minimal wind speed.

One of the major sources of error in this method is the error associated with the creation of surface over the points within each canopy slice along the vertical gradient within a stand. The point cloud density is quite high in terrestrial point cloud datasets used for this study and the point spacing is 2 cm at 20 meters. Creating a

surface using a 5 cm cell size over points that are spaced millimeters apart can potentially overestimate the canopy cover.

## 5. Conclusions

In summary, a robust method for extracting and quantifying plot canopy structure from TLS point clouds has been developed. Canopy structure can be successfully described and compared along the vertical height gradient using patch metrics technique on a classified point cloud surface. The differences in canopy structure derived from TLS point cloud between the plots with varying stand density and biomass can be measured using multivariate analysis techniques. Additionally, we were able to conclude that individual tree measurements such as tree heights, heights to live crown and tree diameter also have a significant effect on the canopy structure of the stand.

Although for this research the focus was predominantly on canopy structure of the stands, the method described in this study can be applied to describe many other spatial distributions within the stand. The slicing and surface creating method accurately captures the spatial distribution of stand parts and quantitatively characterizes the attributes of the stand features on any desirable height gradient with any desirable sampling frequency. One can omit the canopy and slice the stand at the lower height gradients from ground to crown to capture the volume and distribution of understory within the plot. This kind of understory mass quantification is a superior approach to the current method of vegetation transects or sampling square meter subplots that sample a very small part of the plot and then are further extrapolated to the rest of the surface.

## 5.1 Future Research

Terrestrial laser scanner derived canopy structure metrics can be applied in a number of ecological applications. The biggest interest in the use of the proposed method for canopy structure quantification has come from wildlife biologists for wildlife habitat assessment, specifically for protected avian species, like Marbled Murrelet, spotted owl, and canopy dwelling mammals, i.e. red tree voles. The next steps would be to test the canopy structure model in ecological applications and use the canopy metrics to predict nest suitability and stand occupancy by marbled murrelets.

Foregoing the need to model the ground collected variables and treating the canopy variables as unique measures of canopy structure that hold great potential in assessing the habitat suitability, distribution of epiphytes and many more.

## Bibliography

- Antonarakis, A. S., K. S. Richards, J. Brasington, and M. Bithell. 2009. Leafless roughness of complex tree morphology using terrestrial lidar, *Water Resour. Res.* (45): W10401
- Baltsavius, E.P., 1999. Airborne laser scanning: existing systems and firms and other resources. *ISPRS Journal of Photogrammetry and Remote Sensing.* (54):164-198
- Barilotti, A., F. Sepic, E. Abramo. 2008. Automatic detection of dominated vegetation under canopy using Airborne Laser Scanning data. *SilviLaser 2008.* Sept. 17-19. Edinburgh, UK
- Barnes, B.V., Zak, D.R., Denton, S.R., Spurr, S.H. (1998). *Forest Ecology.* John Wiley & Sons, Inc., New York, New York
- Buften, J.L. 1989. Laser altimeter measurements from aircraft and spacecraft. *Proceedings of IEEE.* (77):463-477.
- Campbell, E.M., R.I. Alfaro, and B. Hawkes. 2007. Spatial Distribution of Mountain Pine Beetle Outbreaks in Relation to Climate and Stand Characteristics: A Dendroecological Analysis. *Journal of Integrative Plant Biology.* (2):168-178
- Chapin III, F.S., P.M. Matson, H.A. Mooney. (2002). *Principles of Terrestrial Ecosystem Ecology.* New York, New York, Springer-Verlag.
- Coops, N.C., T. Hilker, M.A. Wulder, B. St-Onge, G. Newnham, A. Siggins, J.A. Trofymow. 2007. Estimating canopy structure of Douglass-fir forest stands from discrete-return LiDAR. *Trees.* (21):295-310
- Cote, J-F., J-L. Widlowski, R.A. Fournier, M.M. Verstraete. 2009. The structural and radiative consistency of three-dimensional tree reconstructions from terrestrial lidar. *Remote Sensing of Environment.* (113)1067-1081
- Cote, J-F., R.A. Fournier, J. E. Luther, O. R. van Lier. 2012. Toward an Enhanced Forest Inventory Using Terrestrial and Airborne LiDAR in Newfoundland: a Virtual Journey through the *L-Architect* Model. *Proceedings of "Silvilaser 2012".* Vancouver, Canada
- Cruz M.G., M.E. Alexander, R.H. Wakimoto. 2003. Assessing canopy fuel stratum characteristics in crown fire prone fuel types of western North America. *International Journal of Wildland Fire.* (12): 39–50.
- Disney, M., P. Lewis, P. Raunonen. 2012. Testing a new vegetation structure retrieval algorithm from terrestrial lidar scanner data using 3D models. *Proceedings of "Silvilaser 2012".* Vancouver, Canada
- Flewelling, J. (ed.), 2012. Panther Creek Field Tour, September 15, 2012, unpublished handout, 71 p. ([http://seattlebiometrics.com/public/pc/pres/2012/tour\\_20120915.pdf](http://seattlebiometrics.com/public/pc/pres/2012/tour_20120915.pdf))

- Franklin, J.F., C.T. Dyrness. 1973. Natural Vegetation of Oregon and Washington. USDA Forest Service General Technical Report PNW-8. Pacific Northwest Forest and Range Experiment Station. Forest Service, US Department of Agriculture.
- Franklin, J.F., Spies, T.A., Van Pelt, R., Carey, A.B., Thornburgh, D.A., Berg, D.R., Lindenmayer, D.B., Harmon, M.E., Keeton, W.S., Shaw, D.C., Bible, K., and Chen, J. 2002. Disturbances and natural development of natural forest ecosystems with silvicultural implications, using Douglas-fir forests as an example. *Forest Ecology and Management*. (155):399-423
- Garcia, M., D. Riano, E. Chuvieco, F.M. Danson. 2009. Estimating biomass carbon stocks for a mediterranean forest in central Spain using LiDAR height and intensity data. *Remote Sensing of Environment*. (114)816-830
- Harding, D.J., M.A. Lefsky, G.G. Parker, J.B. Blair. 2001. Laser altimeter canopy height profiles: Methods and validation for closed-canopy, broadleaf forests. *Remote Sensing of Environment*. (76)283-297
- Hawbaker, T. J., N. S. Keuler, A. A. Lesak, T. Gobakken, K. Contrucci, and V. C. Radeloff. 2009. Improved estimates of forest vegetation structure and biomass with a LiDAR-optimized sampling design, *J. Geophys. Res.*(114): G00E04,
- Hopkinson, C., L. Chasmer, C. Young-pow, and P. Treitz. 2004. Assessing Forest Metrics with a Ground-based Scanning LiDAR. *Canadian Journal of Forest Research*. (34):573-583
- Hopkinson, C.L., J. Lovell, L. Chasmer, D. Jupp, N. Kljun, E. van Gorsel. 2013. Integrating terrestrial and airborne lidar to calibrate a 3D canopy model of effective leaf area index. *Remote Sensing of Environment*. (136):301-314
- Husch, B., Beers, T.W., Kershaw, JR., JA. (2003). *Forest Mensuration*. John Wiley & Sons, Inc., Hoboken, New Jersey
- Hyypä, J., O. Kelle, M. Lehtikoinen, and M. Inkinen. 2001. A segmentation-based method to retrieve stem volume estimates from 3-D tree height models produced by laser scanners. *IEEE Transactions on Geoscience and Remote Sensing*, 39(5):969-975
- Jupp, David L B, D S Culvenor, J L Lovell, G J Newnham, a H Strahler, and C E Woodcock. 2009. "Estimating Forest LAI Profiles and Structural Parameters Using a Ground-based Laser Called 'Echidna'." *Tree Physiology* 29 (2): 171–81.
- Lee, Alex C., and Richard M. Lucas. 2007. "A LiDAR-derived Canopy Density Model for Tree Stem and Crown Mapping in Australian Forests." *Remote Sensing of Environment* 111 (4): 493–518.
- Kelbe, D., P. Romanczyk, J. van Aardt, K. Cawse-Nicholson, and K. Krause. 2012. Automatic extraction of tree stem models from single terrestrial lidar scans in structurally heterogeneous forest environments. Proceedings of "Silvilaser 2012". Vancouver, Canada
- Kimmins, J.P. (1997). *Forest Ecology*. Upper Saddle River, New Jersey, Prentice-Hall, Inc.

- Lefsky, M.A. 1999. Lidar remote sensing of the canopy structure and biophysical properties of Douglas-fir Western hemlock forests. *Remote Sensing of Environment*. 70(3):339-361
- Lefsky, M.A., W.B. Cohen, G.G. Parker, and D.J. Parker. 2002. Lidar Remote Sensing for Ecosystem Studies. *BioScience*. (52)19-30
- Leiterer R., F. Morsdorf, M.E. Schaepman, W. Mucke, M. Hollaus, and N. Pfeifer. 2012. Robust characterization of forest canopy structure using full-waveform airborne laser scanning. Proceedings of "Silvilaser 2012". Vancouver, Canada
- Liang, Xinlian, Paula Litkey, Juha Hyyppa, Harri Kaartinen, Mikko Vastaranta, and Markus Holopainen. 2012. "Automatic Stem Mapping Using Single-Scan Terrestrial Laser Scanning." *IEEE Transactions on Geoscience and Remote Sensing* 50 (2): 661–670.
- Lillesand, T.M., R. W. Kiefer, and J.W. Chipman. 2008. *Remote Sensing and Image Interpretation*. John Wiley and sons, Hoboken, New Jersey
- Lim, K., P. Treitz, K. Baldwin, I. Morrison, and J. Green. 2003a. Lidar remote sensing of biophysical properties of northern tolerant hardwood forests. *Can. J. Remote Sensing*. (29):658-678
- Lim, K., P. Treitz, M. Wulder, B. St-Onge, and M. Flood. 2003b. LiDAR remote sensing of forest structure. *Prog. Phys. Geogr.* (1):88-106
- Lincoln, R., G. Boxshall, and P. Clark. (1998). *A dictionary of ecology, evolution and systematic*. Cambridge, UK., Cambridge University Press
- Lovell, J.L., D.L.B. Jupp, D. Culvenor, and N.C. Coops. 2003. Using airborne and ground based ranging LiDAR to measure canopy structure in Australian forests. *Can. J. Remote Sens.* (29):607-622
- Maier, B., D. Tiede, L. Dorren. 2008. Characterising mountain forest structure using landscape metrics on Lidar-based canopy surface models. *Object-Based Image Analysis Lecture Notes in Geoinformation and Cartography*. Springer. Berlin
- McCune, B. and J.B. Grace, *Analysis of ecological communities*. 2002, Glenden Beach, OR: MjM Software Design.
- McGarigal, K., SA Cushman, and E Ene. 2012. FRAGSTATS v4: Spatial Pattern Analysis Program for Categorical and Continuous Maps. Computer software program produced by the authors at the University of Massachusetts, Amherst. Available at the following web site: <http://www.umass.edu/landeco/research/fragstats/fragstats.html>
- McGaughey, R. J. 2008. FUSION/LDV: software for LIDAR data analysis and visualization, USDA Forest Service, Pacific Northwest Research Station.
- Michel, A.K., and S. Winter. 2009. Tree microhabitat structures as indicators of biodiversity in Douglas-fir forests of different stand ages and management histories in the Pacific Northwest, USA. *Forest Ecology and Management*. (257):1453-1464



- Moskal, L. M. 2010, Panther Creek Terrestrial LiDAR Scanning Final Report for the Bureau of Land Management, University of Washington, Seattle.
- Moskal, L. Monika, and Guang Zheng. 2011. "Retrieving Forest Inventory Variables with Terrestrial Laser Scanning (TLS) in Urban Heterogeneous Forest." *Remote Sensing* 4 (1): 1–20.
- Oksanen, J, F. Guillaume Blanchet, Roeland Kindt, Pierre Legendre, Peter R. Minchin, R. B. O'Hara, Gavin L. Simpson, Peter Solymos, M. Henry H. Stevens and Helene Wagner (2012). *vegan: Community Ecology Package*. R package version 2.0-5. <http://CRAN.R-project.org/package=vegan>
- Parker, G.G., D.J. Harding, and M.L. Berger. 2004. A portable LIDAR system for rapid determination of forest canopy structure. *Journal of Applied Ecology*. (41):755-767
- Parker, G.G., and M.E. Russ. 2004. The canopy surface and stand development: assessing forest canopy structure and complexity with near-surface altimetry. *Forest Ecology and Management*. (189):307-315
- Pueschel, Pyare. 2013. "The Influence of Scanner Parameters on the Extraction of Tree Metrics from FARO Photon 120 Terrestrial Laser Scans." *ISPRS Journal of Photogrammetry and Remote Sensing* 78: 58–68.
- Rapp, V., 2003. New Findings About Old-Growth Forests. PNW Science Update 4. USDA Forest Service PNW Research Station. 11 pp.
- R Core Team. 2012. *R: A Language and Environment for Statistical Computing*. R Foundation for Statistical Computing, Vienna, Austria. <http://www.R-project.org>
- Reineke, L.H. 1933. Perfecting a stand density index for even-age forests. *Journal of Agriculture Research*, (46):627-38
- Rempel, R.S., D. Kaukinen., and A.P. Carr. 2012. Patch Analyst and Patch Grid. Ontario Ministry of Natural Resources. Centre for Northern Forest Ecosystem Research, Thunder Bay, Ontario. [online: <http://www.cnfer.on.ca/SEP/patchanalyst/>]
- Richardson, J.J., L.M. Moskal, S.-H. Kim. 2009. Modeling approaches to estimate effective leaf area index from aerial discrete return LiDAR. *Agricultural and Forest Meteorology*. (149):1152-1160
- Ritchie, J.J., D.L. Evans, D. Jacobs, J.H. Everitt, and M.A. Weltz. 1993. Measuring canopy structure with an airborne laser altimeter. *Transactions of the American Society of Agricultural Engineers*. (36):1235-1238
- RStudio. 2012. *RStudio: Integrated development environment for R (Version 0.96.122)* [Computer software]. Boston, MA. 2012. Available from <http://www.rstudio.org/>
- Schilling, A., A. Schmidt, H.-G. Maas. 2012. Principal Curves for tree Topology Retrieval from TLS Data. Proceedings of "Silvilaser 2012". Vancouver, Canada
- Shroeder, R.L., 1983. Habitat suitability models: blackcapped chickadee. FWS/OBS – 82/10.37. USDI Fish and Wildlife Service, Washington DC

- Sumnall, M.J., R.A.Hill, S.A. Hinsley. 2012. The estimation of forest inventory parameters from small-footprint waveform and discrete return airborne LiDAR data. Proceedings of “Silvilaser 2012”. 1-8, Vancouver, Canada
- Tappeiner II, J.C., D.A. Maguire, T.B. Harrington. (2007). *Silviculture and Ecology of Western U.S. Forests*. Corvallis, Oregon, Oregon State University Press
- Therneau, T.M., Beth Atkinson, Brian Ripley, Jari Oksanen, Glenn De'ath. (2012). mvpart: Multivariate partitioning. R package version 1.6-0. <http://CRAN.R-project.org/package=mvpart>
- Van der Zande D., W. Hoet, I. Jonckheere, J. van Aardt, and P. Coppin. 2006. Influence of measurement set-up of ground-based LiDAR for derivation of tree structure. *Agricultural forest and Meteorology*. (141)147-160
- Van Pelt, R. 2007. *Identifying Mature and Old Forests in Western Washington*. Washington State Department of Natural Resources, Olympia, WA
- Van Pelt, R., N.M. Nadkarni, 2004. Development of Canopy Structure in *Pseudotsuga menziesii* forests in the Southern Washington Cascades. *Forest Science*. (50)326-341
- Van Pelt, R. Sillett, S.C., and N. M. Nadkarni. 2004. Quantifying and visualizing canopy structure in tall forests: Methods and a case study. M. D. Lowman and H. B. Rinker, editors. 2nd edition. *Forest Canopies, Second Edition*. Academic/Elsevier, San Diego.
- Watershed Sciences. 2010. *LiDAR Remote Sensing Data Collection Report: Panther Creek Oregon*. Watershed Sciences, Applied Remote Sensing and Analysis. Portland, Oregon
- Watt, P. J., and D. N. M. Donoghue. 2005. “Measuring Forest Structure with Terrestrial Laser Scanning.” *International Journal of Remote Sensing* 26 (7): 1437–1446.
- Yao, Tian, Xiaoyuan Yang, Feng Zhao, Zhuosen Wang, Qingling Zhang, David Jupp, Jenny Lovell, et al. 2011. “Measuring Forest Structure and Biomass in New England Forest Stands Using Echidna Ground-based Lidar.” *Remote Sensing of Environment* 115 (11): 2965–2974.
- Zheng, G., Moskal L.M., 2012. Computational-Geometry-Based Retrieval of Effective Leaf Area Index Using Terrestrial Laser Scanning. *IEEE Transactions on Geoscience and Remote Sensing*. 50(10):3958-3969

## Appendix A: List of acronyms

ASCII:	American Standard Code for Information Interchange
BLM:	Bureau of Land Management
GIS:	Geographic Information Systems
GPS:	Global Positioning System
LiDAR:	Light Detection and Ranging
TLS:	Terrestrial Laser Scanning
ALS:	Aerial Laser Scanning
OBIA:	Object Based Image Analysis
CHM:	Canopy Height Model
SDI:	Stand Density Index
TPH:	Trees Per Hectare
BA:	Basal Area
MPAR:	Mean Perimeter to Area Ratio
AGB:	Aboveground Biomass
ANOVA:	Analysis of Variance
MANOVA:	Multiple Analysis of Variance
SEI:	Shannon's Evenness Index
CM:	Canopy Mass
MPFD:	Mean Patch Fractal Dimension
AWMSI:	Area Weighted Mean Shape Index
MSI:	Mean Shape Index
PPSD:	Patch Size Standard Deviation
SDI2:	Shannon's Diversity Index

## Appendix B: List of definitions

*Stand structure* – spatial (vertical and horizontal) arrangement of vegetation individuals in a stand.

*Plant community composition* – a list of the species that comprise a community or any other ecological unit.

*Aboveground tree biomass* – quantity of aboveground living material stored in the trees within a system.

*Active remote sensing* – remote sensing that uses sensors that detect reflected responses from objects that irradiated from artificially-generated energy sources, such as radar or LiDAR.

*Passive remote sensing* – remote sensing that makes use of sensors that detect the reflected or emitted electromagnetic radiation from natural sources.

*Airborne Laser Scanner (ALS)* – an optical remote sensing technology that measures properties of scattered light to find range and/or other information of a distant target.

*Point cloud* – is a set of vertices in a three-dimensional coordinate system. The vertices are usually defined by X, Y, and Z coordinates, and are typically intended to be representative of the external surface of an object.

*Classification (Object-oriented)* – a procedure that categorizes an image into classes or themes that involves both spectral and spatial pattern recognition.

*Object based image analysis (OBIA)* – is a method of classification involving the delineation (segmentation) of similar pixels into a discrete objects and is followed by the classification of those objects into themes or classes.

*Landscape metrics* – indices developed for categorical map patterns. Landscape metrics are algorithms that quantify specific spatial characteristics of patches, classes of patches, or entire landscape mosaics.

*TLS* – Terrestrial laser scanning

*Richness* – the number of different patch types

*Evenness* – is the relative abundance of different patch types, emphasizing either relative dominance or its compliment, equitability.

LiDAR – An active sensor that records distance based on emitted laser pulses.

LiDAR intensity - the strength of the LiDAR return signal off of a surface.

## Appendix C: Metadata

### *Patch Metrics Code names:*

SDI = Shannon's Diversity Index  
 SEI = Shannon's Evenness Index  
 AWMSI = Area Weighted Mean Shape Index  
 MSI = Mean Shape Index  
 MPAR = Mean Perimeter to Area Ratio  
 MPFD = Mean Patch Fractal Dimension  
 AWMPFD = Area Weighted Mean Patch Fractal Dimension  
 TE = Total Edge  
 ED = Edge density  
 MPE = Mean Patch Edge  
 MPS = Mean Patch Size  
 NumP = number of patches  
 MedPS = Median Patch Size  
 PSCov = Patch Size Coefficient of Variance  
 PSSD = Patch Size Standard Deviation  
 TLA = Total Landscape Area  
 CA = Class Area

### *Coding of Environmental Matrix Variables*

PLOT = plot #  
 St.type = stand type, 1 or 2, where 1=Doug Fir and 2=Mixed  
 Tr.number = number of trees in plot  
 TPH = trees per hectare  
 c.mass = Canopy density (kg) – canopy biomass from biopak formula

Agb = above ground biomass (t/ha), total mass within the plot (tree mass) from biopak formula  
 Qmd = (cm) – Quadratic Mean Diameter, where  $QMD = \sqrt{(\sum d_i^2/n)}$ , where  $d_i$ -observed diameter, n-observed number of trees per unit area

Sdi = SDI (Stand Density Index) – or Reineke's (1933) stand density index – function of quadratic mean diameter and number of trees per unit area  $SDI = N_o(D_o/10)^{1.605}$ , where  $N_o$  – observed number of trees per unit area,  $D_o$  – observed quadratic mean diameter.

avg.hgt = average tree height (m)  
 avg.hlc = average height to live crown (m)  
 Ba = Basal Area ( $m^2/ha$ ) –  $BA_{(plot)} = \sum BA_{(tree)} / A_{(plot)}$ , where  $BA_{(tree)}(m^2) = 0.00007854 * DBH^2(cm)$

### *Cloudmetrics:*

A. (All returns above 3 meters)/(Total first return) \*100

- B. First returns above 3m
- C. All returns above 3m
- D. Percent of 1<sup>st</sup> returns above the mean
- E. Percent of 1<sup>st</sup> returns above the mode
- F. Percent all returns above the mean
- G. Percent all returns above the mode
- H.  $(\text{All returns above the mean})/(\text{Total first returns}) * 100$
- I.  $(\text{All returns above the mode})/(\text{Total 1}^{\text{st}} \text{ returns}) * 100$
- J. 1<sup>st</sup> returns above the mean
- K. 1<sup>st</sup> return above the mode
- L. All returns above the mean
- M. All returns above the mode
- N. Total 1<sup>st</sup> returns
- O. Total all returns